Molecular signatures and associated regulators of the pea leaf response to sulfur deficiency and water deficit as revealed by multi-omics analyses

Titouan Bonnot[1], Charlotte Henriet[1], Delphine Aimé[1], Jonathan Kreplak[1], Morgane Térézol[1§], Thierry Balliau[2], Alain Ourry[3], Michel Zivy[2], Vanessa Vernoud[1,*] and Karine Gallardo[1,*]

[1] Agroécologie, INRAE, Institut Agro, Univ. Bourgogne, Univ. Bourgogne Franche-Comté, F-21000 Dijon, France

[2] Plateforme d'Analyse de Protéomique Paris Sud-Ouest (PAPPSO), Université Paris-Saclay, INRAE, CNRS, AgroParisTech, UMR Génétique Quantitative et Évolution-Le Moulon, 91190 Gif-sur-Yvette, France

[3] UMR 950 Ecophysiologie Végétale, Agronomie et Nutritions N, C, S, Normandie Université, UNICAEN, INRAE, Caen, France

[§] Present address: Aix Marseille Univ, INSERM, MMG, Marseille, France

* These authors contributed equally

Corresponding author: titouan.bonnot@inrae.fr

Abstract

Sulfur availability in soils affects both yield and seed quality in major crops, and the plant capacity to tolerate environmental constraints. Under stress combination, plants often show specific responses at the molecular level. To dissect the molecular responses to sulfur deficiency in interaction or not with water deficit, a multi-omics approach was used focusing on the leaves of pea (*Pisum sativum*), at several days during the early reproductive phase. Using ionomics, transcriptomics, proteomics and gene network analyses, we identified a module of genes strongly driven by sulfur availability. This includes known and putative new players of plant responses to sulfur-deprived conditions. Conserved profiles between proteins and mRNAs were specifically observed within this module, suggesting transcriptional regulation. While moderate water deficit had little impact when occurring alone, it thoroughly perturbed plant growth and the leaf transcriptome and proteome when combined with sulfur deficiency. Under this stress combination, molecular responses were amplified, notably at the transcriptome level, in a time-specific manner. Genes with specific or

greater responses under this condition were identified, and transcriptional regulators of the highlighted genes and pathways were predicted, which may represent interesting targets to develop crops tolerant to multi-stress conditions.

Introduction

Human activities are responsible for global changes such as global warming and climate change, some of which are now inevitable and irreversible (IPCC 2023). Besides an increase in both the intensity and frequency of extreme events, the number of factors and their interactions, that affect ecosystem functioning, are growing rapidly (Paine et al. 1998; IPCC 2023). In the field, plants can face multiple growth-limiting stresses that can occur sequentially or simultaneously, such as elevated temperatures and water deficit (WD), or WD and nutrient deficiencies (Mittler 2006; Lecomte et al. 2023). Combination of stresses can have a more dramatic impact on crop yields than individual stress conditions, as observed under combined heat stress and drought or under drought and sulfur (S) deficiency (Henriet et al. 2019; Cohen et al. 2021). At the molecular level, previous studies performed in controlled or semi-controlled conditions revealed that combination of stresses often resulted in unique molecular signatures, that could not be predicted by studying the plant responses to each individual stress (Rizhsky et al. 2002, 2004; Mittler 2006; Rasmussen et al. 2013; Zandalinas et al. 2021; Mahalingam et al. 2022; Tan et al. 2023). For example, ~55% of genes responding to heat and/or drought stress in Arabidopsis showed antagonistic or synergistic responses under combined heat stress and drought (Azodi et al. 2020). Such specificities may reflect the activation of unique biological pathways that are critical for the plant tolerance to a given combination of stresses (Zandalinas et al. 2021), and need to be considered for improving the tolerance to environmental constraints. While extensive work has been done to study plant responses to a wide variety of single stress treatments, little is still known about responses to multi-stress conditions in crops, especially at the molecular level (Zandalinas and Mittler 2022).

To limit global warming to the most optimistic scenarios, deep and rapid cuts in greenhouse gas emissions are needed (IPCC 2023). Increasing the cultivation of pulses – which generates little CO_2 as compared to the production of other major foods (Poore and Nemecek 2018) – would contribute to this effort. Moreover, the capacity of legume species to fix atmospheric N_2 through root nodule symbiosis allows them to accumulate high amounts of proteins in seeds without the need of nitrogen (N)

fertilization, which makes them interesting protein-rich alternatives to animal-based foods (Stagnari et al. 2017; Detzel et al. 2022). Although recent advances in the development of genomic tools and technologies have allowed an acceleration of breeding programs in legumes (Varshney et al. 2019), environmental constraints such as abiotic stresses represent major limiting factors for yield potential in species such as pea (*Pisum sativum* L.; Lecomte et al. 2023). A better understanding of the molecular responses of pulses to multi-stress conditions is therefore needed.

Sulfur starvation in soils is reported worldwide, due to several factors such as stricter regulations on industrial SO_2 emissions and the declining use of S-containing pesticides and S fertilizers. This results in S deficiency symptoms in crops, and affects both yield and seed quality (Scherer 2001; Haneklaus et al. 2008; Poisson et al. 2019; Borja Reis et al. 2021). In pea seeds, but also in cereals like wheat, the balance between S and N strongly influences storage protein composition, a key determinant of seed quality (reviewed in Mondal et al. 2022; Bonnot et al. 2023). Previous work in Arabidopsis has revealed genes that are activated under S-deficient conditions, including a set of genes co-expressed with O-acetylserine (OAS) accumulation, known as the OAS cluster genes (Hubberten et al. 2012; Aarabi et al. 2016, 2021). Several members of the OAS cluster are also induced in wheat and pea seeds under S-deficient conditions (Bonnot et al. 2020; Henriet et al. 2021). Some studies suggest a role of this cluster in S sensing and signaling (Ristova and Kopriva 2022). Since S is essential for the synthesis of several antioxidant molecules like glutathione, S- also alters the plant capacity to cope with other environmental constraints (Samanta et al. 2020). However, connections between known regulatory genes of the plant response to S-limiting conditions and of pathways of response to abiotic stresses are still unclear.

We previously investigated the interaction between S- and WD during the early reproductive phase in pea (Henriet et al. 2019, 2021), and showed that the combination of the stresses negatively impacted seed yield and seed size in a synergistic manner (Henriet et al. 2019). However, WD mitigated the impact of S- on the seed storage protein composition, suggesting that under stress combination, pea plants employed a strategy to produce fewer seeds with a well-balanced protein composition (Henriet et al. 2019, 2021). At the molecular level, fewer transcripts and proteins were differentially accumulated in developing seeds when the two stresses were combined, as compared to S-. In fact, the response of developing pea seeds to S- in combination with WD depends on a small number of proteins with important protective functions against

oxidative damage or in repair processes. This led us to speculate that most molecular responses activated under combined WD and S- may have occurred in other tissues, in particular in leaves that are a rich source of nutrients for the developing seeds.

To further dissect the molecular pathways activated under WD and S-, we used a multi-omics approach focusing on pea leaves. Transcriptomics, proteomics and ionomics data were obtained at different time points during stresses applied individually or in combination, on leaf samples collected from the experiment described in Henriet et al. (2019, 2021). A highly specific module of genes responding to S- (occurring alone or in combination with WD) was revealed, with known and putative new regulators of the plant's responses to this stress. Our results also emphasized that combination of S- and WD induced specific or amplified responses as compared to single stress conditions. Besides a critical impact on the plant phenotype, the combined stress thoroughly perturbed the leaf transcriptome, proteome and ionome. The transcriptome remarkably responded to this condition, in a time-specific manner. Network analyses allowed us to identify molecular signatures that are specific to this condition and to predict potential regulatory genes of selected modules.

Results

Water deficit combined with S deficiency severely affects the plant growth

To explore the interplay between WD and S-, plants were exposed to either S- starting three weeks after sowing (5/6 leaf stage), moderate WD (50% of the water holding capacity of the substrate) applied at the beginning of flowering for nine days, or to the combination of WD and S- (WD/S-, Figure 1A). The S- treatment was applied 16 days before WD, to ensure that leaf S content was perturbed before water stress imposition. The experimental setup is detailed in (Henriet et al. 2019, 2021). Phenotypic variables were measured in different plant compartments, and leaves of the first two reproductive nodes were collected from control and stressed plants at days 0 (for control and S- conditions only), 2, 5, 9 and 12 to conduct -omics analyses (Figure 1; Supplemental Data Set S1). For conditions WD and WD/S-, day 12 corresponds to three days of rewatering, and informs on the plant recovery after WD. Separate statistical analyses were performed for data obtained at day 0 and day 12 due to different treatment modalities compared to the other time points (see methods). Few effects of WD applied alone on the measured traits were observed (Figure 1B; Supplemental Data Set S2). The only significant changes were a decrease in the dry weight of leaves from the

reproductive part of the plant at day 12 (Figure 1B; Supplemental Data Set S1), and a lower osmotic potential at day 5 (-1.34 MPa under WD, -1.21 MPa under control conditions, $P \approx 2.8E\text{-}03$; Figure 1C; Supplemental Data Sets S1 and S2).

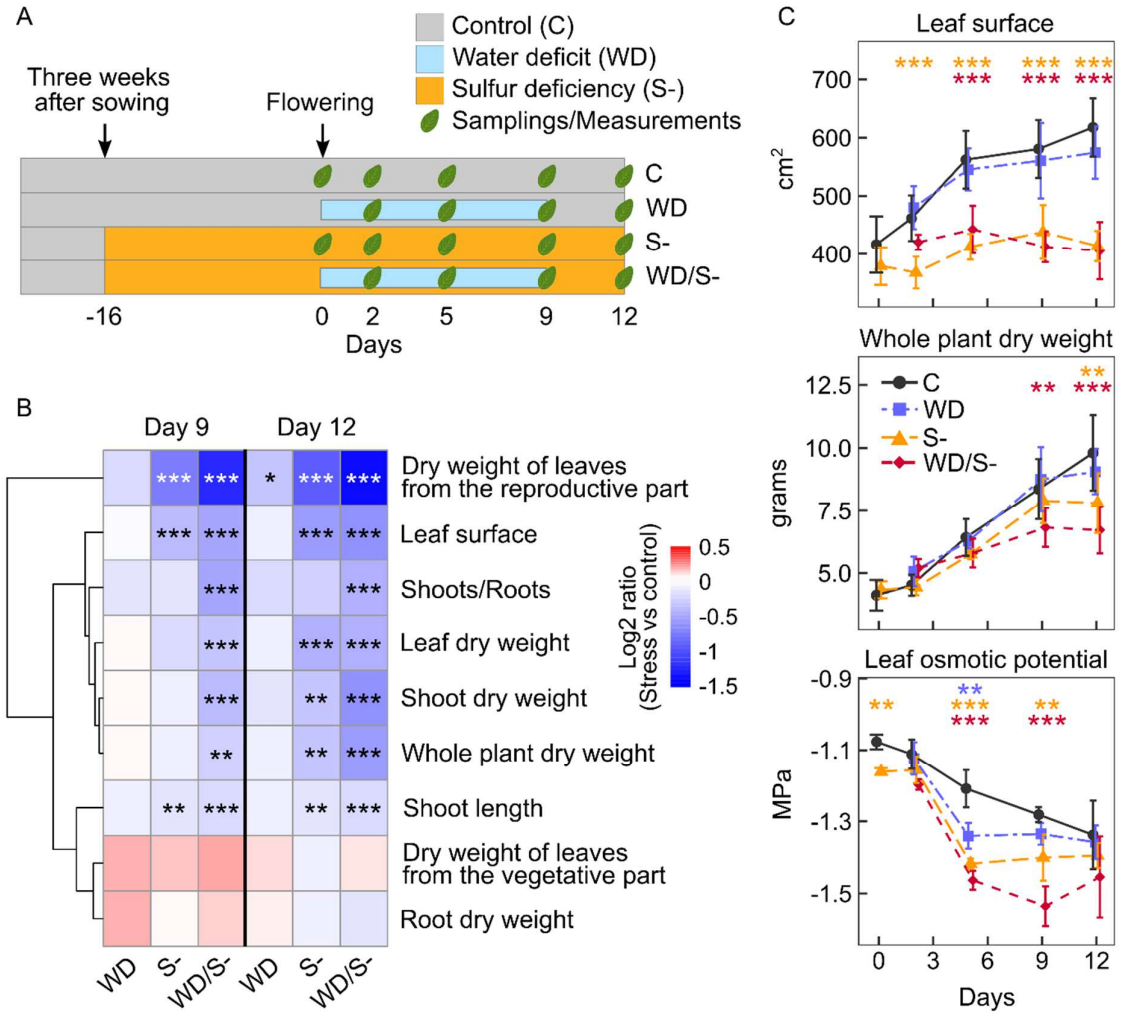

Figure 1. Influence of water deficit (WD), sulfur deficiency (S-) and combined stresses on pea plant phenotypic variables. A, Experimental design. Days 0 and 9 correspond to the beginning and end of WD, respectively. For the conditions WD and WD/S-, day 12 corresponds to three days of rewatering for plant recovery. B, Effects of stresses on phenotypic variables, at the end of the WD stress imposition (day 9) and after three days of rewatering (day 12). Data are represented as heatmaps, blue and red representing lower and higher values in the stress condition as compared to control, respectively. Variables with similar responses to stress are grouped using a hierarchical clustering method. Data are means ± S.D. of $n = 8$ biological replicates (eight individual plants per condition). Raw data are presented in Supplemental Data Set S1. C, Profile of leaf surface, whole plant dry weight and leaf osmotic potential. Data are means ± S.D. of $n = 8$ (surface and weight) or n=4 (osmotic potential) biological replicates. In B and C, asterisks indicate significant differences between stress and control conditions (*, $P < 0.05$; **, $P < 0.01$; ***, $P < 0.001$). In C, orange, blue and red asterisks refer to S-, WD and WD/S- conditions, respectively. Three separate statistical analyses were performed: comparison of S- and control at day 0 (Student's t-test); comparisons of all treatments from day 2 to day 9 (two-way ANOVA); comparisons of all treatments at day 12 during the plant recovery (one-way ANOVA, see methods for details).

Under S-, several plant traits were affected, with a significant reduction in leaf surface, shoot length, and in leaf, shoot and whole plant dry weight (Figure 1, B and C; Supplemental Data Set S2). Together with a significant reduction in the leaf osmotic potential (days 0, 5 and 9), these results highlighted the negative impact of S- on the plant development and physiology (Figure 1C; Supplemental Data Set S2). Of note, the significant reduction of the leaf osmotic potential at day 0 under S- indicates that our S deficiency treatment induced a stress before the WD imposition.

When the two stresses were combined (WD/S-), the plant height, the leaf surface area, the plant biomass and the shoot-to-root ratio were strongly affected (Figure 1, B and C). This was observed at both day 9, when stress intensity was the highest, and at day 12, *i.e.* three days after plant rewatering (Figure 1B). For example, at day 12, the leaf surface area and the whole plant dry weight were reduced by 34.3% ($P \approx$ 6.14E-09) and by 31.5% ($P \approx$ 6.14E-05), respectively (Figure 1, B and C; Supplemental Data Sets S1 and S2). Measurements of the leaf osmotic potential confirmed the amplified effect induced by the stress combination, with the lowest osmotic potential value measured at day 9 under WD/S- (-1.54 MPa, Figure 1C; Supplemental Data Set S1). Taken together, these results showed that while the WD treatment had moderate effects compared to S-, it severely affected plant growth when combined with S-.

Nutrients and potentially toxic elements show specific accumulation profiles in response to single and combined stress treatments

To estimate the impact of the single or combined stresses on the plant nutritional status, we next quantified the carbon (C), N and S contents in leaves using the Dumas method (Supplemental Data Set S1). No significant differences were observed in response to WD applied alone, although leaf N content tends to be lower under this condition (Figure 2A). Both S- and WD/S- treatments significantly reduced leaf C, N and S contents at one or more time points (Figure 2A; Supplemental Data Set S2). At day 0, all three elements were significantly less accumulated in response to S- (Figure 2A), indicating that the leaf elemental composition was altered even before WD imposition, as expected from our experimental design where S- was applied at the 5/6 leaf stage, *i.e.* about 16 days before the onset of WD. S-deficient treatments (S- and WD/S-) remarkably impacted S content in leaves, which dropped from 0.23% of the leaf dry weight (on average, from day 2 to day 12) in control condition to 0.090% and 0.087% in response to S- and WD/S-, respectively (Figure 2A; Supplemental Data Set

S1). With no clear distinction between control and WD, or between S- and WD/S-, this highlights that our S- treatment strongly reduced S accumulation and/or transport in pea leaves, regardless of water supply. Changes in C, N and S contents under stress therefore altered the balance between these elements in leaves, especially the N/S ratio, which highly increased under both S- and WD/S- (Figure 2A).

To further evaluate the perturbations induced by stresses on the plant nutrition, we extended our analyses to other essential macro-nutrients (phosphorus, potassium, calcium, magnesium), micro-nutrients (iron, boron, manganese, zinc, copper, molybdenum, nickel) and other elements (cobalt, cadmium, lead, arsenic, vanadium) using high-resolution inductively coupled plasma mass spectrometry (HR ICP-MS, Figure 2B; Supplemental Data Set S1; Supplemental Figure S2). This analysis also included the quantification of S, which showed very consistent results as those obtained with the Dumas method (R = 0.9; Supplemental Figure S1). Molybdenum showed remarkable higher contents in leaves under S- and WD/S- as compared to control and WD conditions at all time points, and was strongly correlated with S content (R = -0.78) and N/S ratio (R = 0.85) variables (Figure 2, B and C).

All macro- and micro-nutrients, except molybdenum and nickel, were less accumulated in leaves under S- as compared to control (Figure 2B; Supplemental Figure S2), suggesting that S deprivation altered the uptake and transport of other nutrients in leaves, as previously reported in pea (Jacques et al. 2021). Significant reduced accumulation of S in leaves was also observed under WD at day 2 (Figure 2B; Supplemental Figure S2; Supplemental Data Set S2). In response to WD, accumulation of iron, magnesium and zinc in leaves tended to increase, and this increase was even more pronounced when plants were exposed to WD/S-, especially from days 5 to 12 (Figure 2B; Supplemental Figure S2). While iron and zinc are two essential micro-nutrients, they become toxic at high concentration (Connolly and Guerinot 2002; Balafrej et al. 2020). Similarly, hyperaccumulation of cobalt, specifically observed at day 9 under WD/S- and during recovery at day 12 (Figure 2B; Supplemental Figure S2), can be detrimental to plants (Hu et al. 2021). Non-essential elements that can cause deleterious effects on plant growth, such as arsenic and cadmium, were also more accumulated in response to WD/S- (Figure 2B; Supplemental Figure S2). Increased accumulation of cadmium in leaves was also detected in response to S-, specifically from day 0 to day 5 (Supplemental Figure S2).

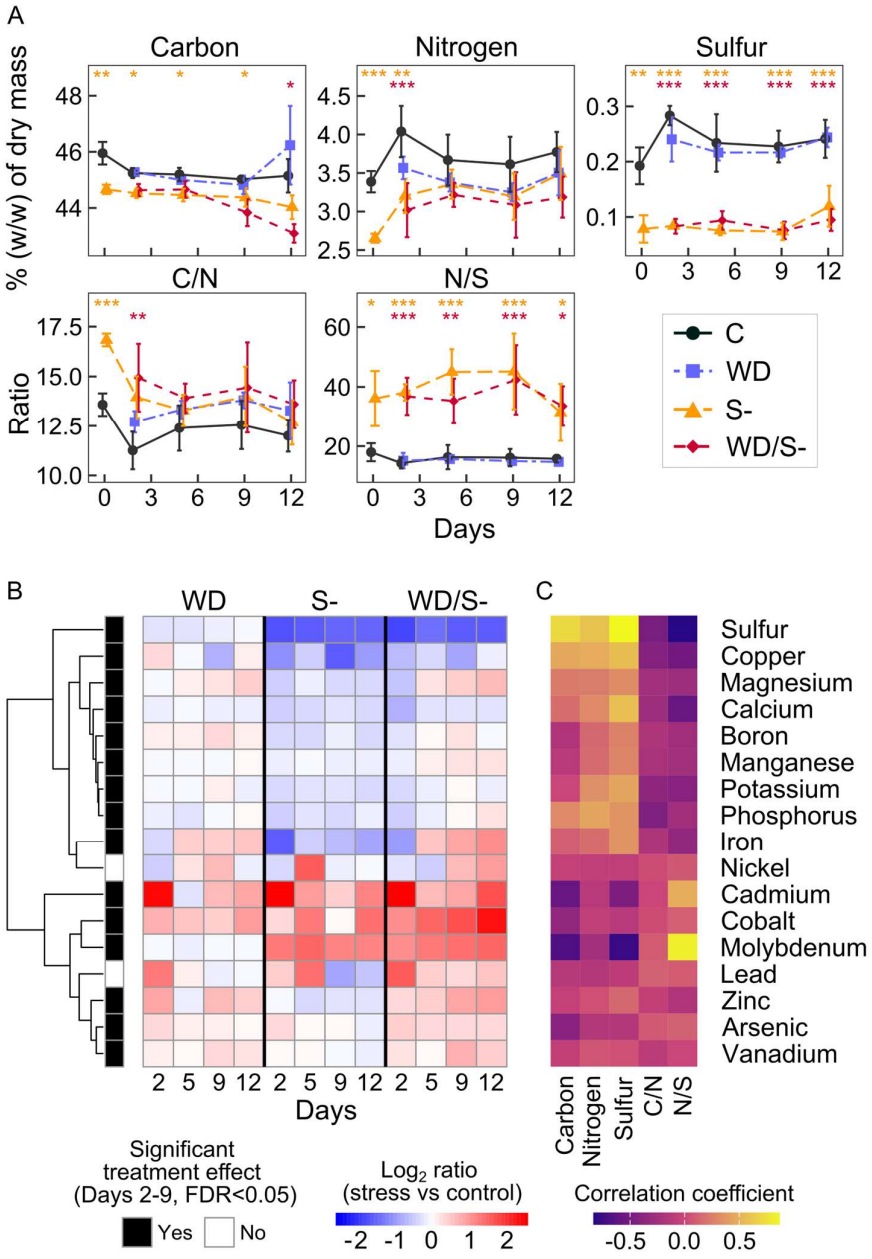

Figure 2. Elemental composition of elements in pea leaves in response to water deficit (WD), sulfur deficiency (S-) and combined stress. A, Profiles of accumulation of Carbon (C), Nitrogen (N), Sulfur (S), as well as C/N and N/S ratios (means ± S.D, *n* = 4 biological replicates). Asterisks indicate significant differences between stress and control conditions (*, P < 0.05; **, P < 0.01; ***, P < 0.001). Orange and red asterisks refer to S- and WD/S- conditions, respectively. Three separate statistical analyses were performed: comparison of S- and control at day 0 (Student's t-test); comparisons of all treatments from day 2 to day 9 (two-way ANOVA); comparisons of all treatments at day 12 during the plant recovery (one-way ANOVA, see methods for details). B, Heatmap representing the change in leaf dry matter content of elements in response to stresses. Blue and red colors represent lower and higher values in the stress condition as compared to control, respectively. Elements with similar profiles are grouped using a hierarchical clustering method. Elements with a significant treatment effect (FDR < 0.05, ANOVA) during the period from day 2 to day 9 are highlighted with a black square. Raw data are provided in Supplemental Data Set S1 and statistical results (including comparison of treatments at day 12) are in Supplemental Data Set S2. C, Heatmap of Spearman correlation between element content and variables presented in A. Yellow and purple colors represent positive and negative correlation coefficients, respectively.

Taken together, these results showed that stress treatments, especially when combined, led to the accumulation of elements which can compromise plant growth and survival. Zinc, iron and cobalt were particularly accumulated in leaves under WD/S- and therefore represent markers of the combined stress condition, whereas S content, N/S and molybdenum are more specific indicators of S- combined or not with WD.

Stress combination thoroughly perturbs the leaf transcriptome and proteome

To identify genes and biological pathways that are regulated under WD and/or S- and that could be important for the plant tolerance to these stresses, we explored the responses at the transcriptome and proteome levels, using RNA-Sequencing and shotgun proteomics, respectively. In total, 29572 genes were considered as expressed in the experiment (see Methods) and 2261 proteins were successfully quantified (Figure 3A; Supplemental Data Set S3). Since day 12 corresponds to the recovery period after WD, omics data obtained at this time point were statistically analyzed separately (Figure 3A, see Methods).

First, analyses of variance at days 2-9 revealed that the treatments significantly (FDR < 0.05) altered the expression of 14497 (49%) genes and the accumulation of 1327 (58.7%) proteins (Figure 3A; Supplemental Data Set S2). The analysis from days 2-9 also highlighted that 33.6% of the transcriptome showed a significant time × treatment interaction effect, meaning that responses to treatments are influenced by time for these genes (Figure 3A). This proportion was much lower at the proteome level (3.4%), suggesting smaller variations in the stress response over time for proteins. We therefore asked to what extent effects of the stresses on the transcriptome were conserved at the protein level. To this aim, we compared the protein and mRNA profiles of the 2240 genes analyzed in both datasets (Supplemental Data Set S4). Considering the whole datasets (all treatments combined, day 2 to day 12), correlations between mRNAs and proteins ranged from -0.67 to 0.92, with a median at 0.12 (Figure 3B). This overall low correlation indicates that post-transcriptional regulations may strongly influence mRNA translation for a large proportion of the 2240 genes. A similar analysis performed for each treatment showed comparable trends, excluding a potential effect of stresses on the overall correlation between mRNA and protein profiles (Figure 3C). Nonetheless, we identified a group of 308 genes (13.7%) with a correlation greater than 0.5, which are involved in the

biosynthesis of S-containing molecules (Met, Cys, glutathione), and in the response to various stresses including cadmium and oxidative stress (Figure 3, B and D; Supplemental Data Sets S4 and S5). These genes exhibiting higher correlations between their mRNA and protein profiles may be more strongly regulated at the transcriptional level than at the post-transcriptional level.

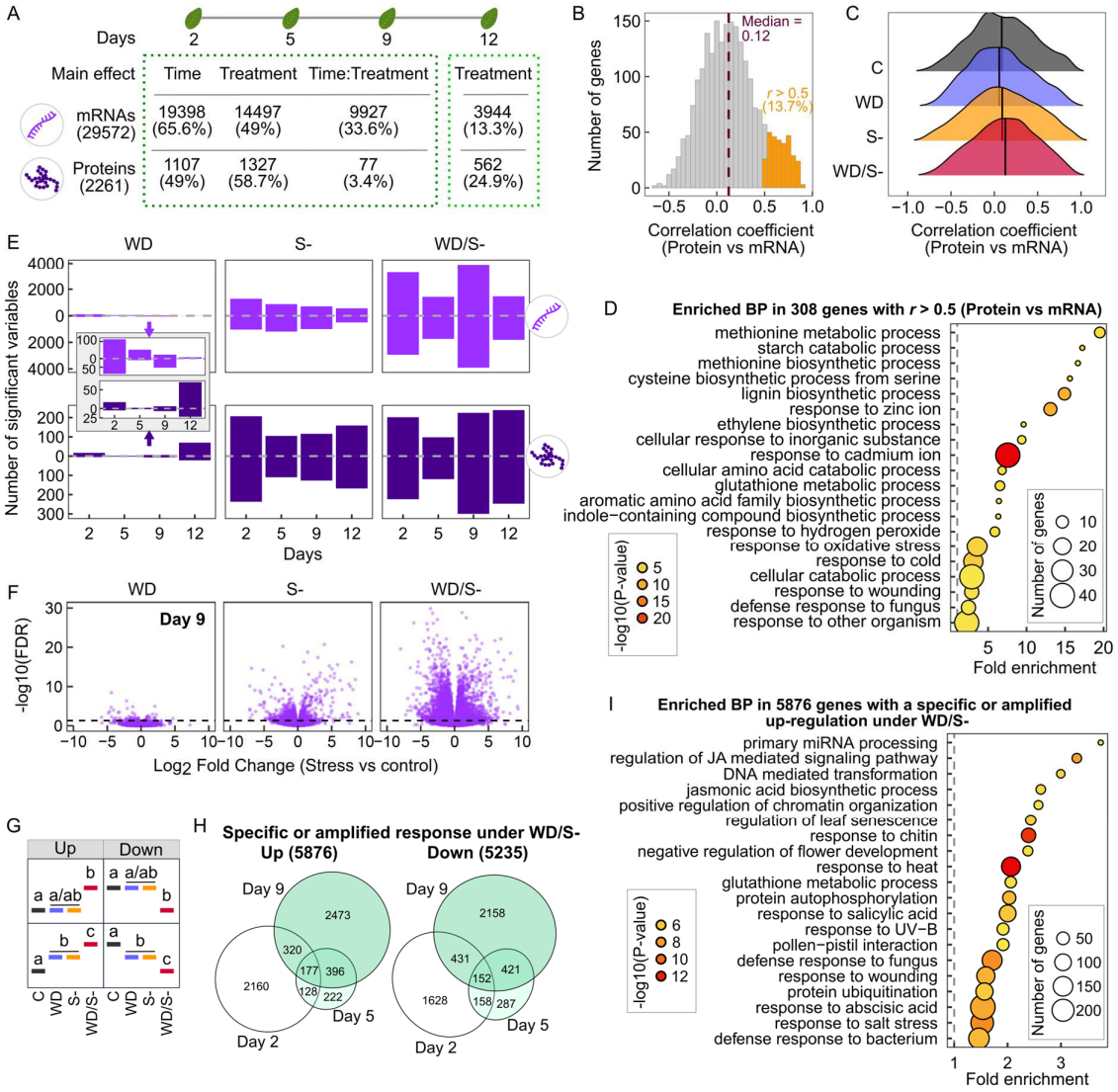

Figure 3. Transcriptome and proteome responses to stress reveal genes with specific or amplified responses under combined stress condition. A, Results of statistical analyses showing the number of mRNAs and proteins with a significant (FDR < 0.05) effect of time, treatment, and the interaction between time and treatment (Time:Treatment). Two separate analyses were performed, one for day 2 to day 9, for which conditions were the same (Two-way ANOVA), and one for day 12, during the plant recovery following WD (One-way ANOVA). The percentage of analyzed molecules with a significant effect is indicated in parentheses (*e.g.* the accumulation of 49% of the proteome is significantly affected by time). B, Histogram showing the distribution of correlation (Spearman) coefficients for the comparisons between proteins and mRNAs (data obtained at days 2, 5, 9 and 12 from all treatment conditions). Genes with a $r > 0.5$ (protein vs mRNA) are highlighted in orange. C, Ridgeline plots showing

the distribution of correlation (Spearman) coefficients for the comparison between proteins and mRNAs, for each condition (conditions were separated for the calculation of correlation coefficients). Vertical black lines indicate medians. In total, 2240 genes were analyzed at both transcriptomic and proteomic levels, and were therefore considered for the analyses shown in B and C. D, Selected enriched biological processes in genes with a $r > 0.5$ (protein vs mRNA) identified in B. The top 20 enriched GO terms (based on P-values) with at least five genes are represented. E, Barplots showing the numbers of differentially accumulated mRNAs and proteins in response to the stress conditions as compared to control, at each developmental stage. This results from pairwise comparisons following the analysis presented in A (variables with a significant treatment effect were used for pairwise comparisons). For WD, zoomed plots are shown to reveal differences between time points. F, Volcano plots representing statistical significance (-log10[FDR]) versus magnitude of change (Log_2 Fold Change) for mRNAs at Day 9. G, Schematic plot summarizing situations where mRNAs were considered as having a specific or amplified response in the combined stress as compared to single stress conditions. H, Venn diagrams depicting the overlap between lists of genes identified at days 2, 5 and 9 with a specific or amplified response in the combined stress condition. I, Selected enriched biological processes in genes with a specific or amplified up-regulation under WD/S- as compared to single stress conditions. The top 20 enriched GO terms (based on P-values) are represented.

Second, pairwise comparisons performed on variables with a significant treatment effect (FDR < 0.05) revealed that many more mRNAs and proteins were differentially accumulated in response to S- and WD/S- than to WD applied alone (Figure 3E; Supplemental Data Set S2). The number of differentially accumulated molecules also differed depending on the days (Figure 3E). For instance, under WD/S-, 3286, 1430 and 3901 genes and 202, 98 and 225 proteins were up-regulated at days 2, 5 and 9, respectively (Figure 3E). Thus, more than twice less genes and proteins were up-regulated at day 5 under WD/S- compared to day 2 or day 9. The influence of time is stronger under WD and WD/S- than under S-, which could be explained by our experimental design, where S deficiency was applied earlier in the plant development as compared to WD (Figure 1A). The transcriptome and proteome reprogramming at day 9 was specifically observed under WD/S-, and may be associated with an intense stress response. Indeed, we observed that S-deficient plants did not survive to a prolonged period of WD (leaves of plants experiencing 12 days of combined stress dried out, Henriet et al., 2019).

Third, we observed that numbers of differentially expressed genes (DEGs) and, to a lesser extent, of differentially accumulated proteins, were larger under WD/S- than under single stresses (Figure 3E). At the transcriptome level, both lower P-values and higher fold change values were observed under this condition (Figure 3F; Supplemental Figure S3). For instance, at day 9, 3901 up-regulated DEGs were identified under WD/S-, whereas only 23 and 709 genes were up-regulated in response to WD and S-, respectively (Figure 3E). To explore this greater response under stress combination, we isolated genes between day 2 and day 9 with either 1) a specific

response under WD/S- (and not under WD or S-, upper panel, Figure 3G), or 2) a greater response under WD/S- as compared to single stress conditions (lower panel, Figure 3G). In total, we identified 5876 up-regulated and 5235 down-regulated DEGs with a specific or amplified response under WD/S- (Figure 3H; Supplemental Data Set S6). The up-regulated DEGs were enriched in genes involved in the response to diverse stresses (*e.g.* heat, UV-B, salt, wounding, fungus), in the response or biosynthesis of hormones (jasmonic acid, salicylic acid, abscisic acid), in epigenetic-related processes (primary miRNA processing, positive regulation of chromatin organization), in glutathione metabolic process and protein modification (autophosphorylation, ubiquitination; Figure 3I; Supplemental Data Set S5). On the contrary, down-regulated DEGs have a role in photosynthesis, photorespiration, phototropism and gravitropism, as well as in translation or response to cold (Supplemental Figure S4, Supplemental Data Set S5). Interestingly, the lists of DEGs with a specific or amplified response were very different depending on the day, with for example 2160 (37%) and 2473 (42%) of the up-regulated DEGs that were specific to day 2 and day 9, respectively (Figure 3H). This result shows that a sequential response is observed under WD/S-, with two waves of response involving different sets of genes.

Co-expression network analysis identifies treatment-driven modules with contrasted patterns of response

To further investigate the influence of treatments on gene expression in leaves and to identify genes with specific patterns of response across development, we employed a weighted-gene co-expression network approach, from data obtained at the transcriptome level using all expressed genes (genes with low expression were not considered, see Methods). This allowed us to build a network composed of 27 modules with different sizes (ranging from 58 to 3970 genes) and with distinct expression patterns (Figure 4, A and B; Supplemental Figure S5; Supplemental Data Set S7).

Within each individual module, we looked for genes with a significant time, treatment, or time × treatment interaction effect (described in Figure 3A) or with a specific or amplified response under WD/S- (identified in Figure 3H). We also explored the repartition of transcriptional regulators within modules, after annotating them using PlantTFcat (Supplemental Data Set S8). An enrichment analysis revealed 12 modules that were significantly enriched for genes with a treatment effect (Figure 4C), which we

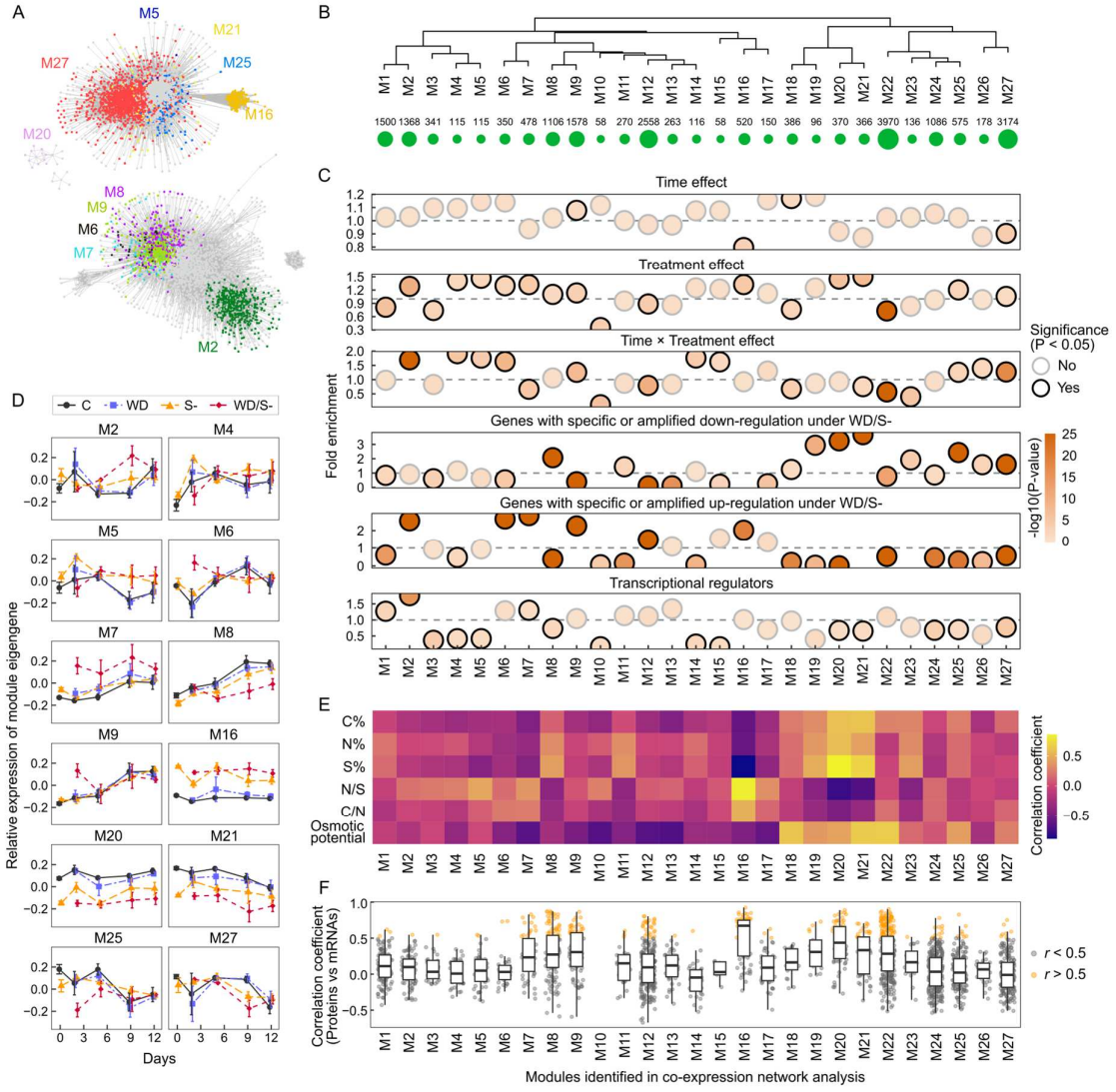

Figure 4. Identification of treatment-driven modules with specific patterns of response to stress using a co-expression network analysis. A, Co-expression network generated with WGCNA and visualized in Cytoscape using a Prefuse Force Directed layout, with an edge threshold cutoff of weight > 0.15. This network was built from transcriptomics data. Colored modules correspond to treatment-driven modules identified in C and presented in D. B, Clustering of module eigengenes. The module eigengene is defined as the first principal component of a given module (Langfelder and Horvath, 2008). The number of genes assigned to each module is indicated below the module name and represented as a bubble plot. C, Bubble plots representing enrichment of specific groups of genes within each module. Fold enrichment < 1 and > 1 correspond to an under- and over-representation in the module, respectively. Significance ($P < 0.05$, Fisher's exact test) is indicated as bubbles circled in black. Genes with a time, treatment and/or time × treatment interaction effects were identified in Figure 3A. Genes with a specific or amplified response in WD/S- at one or more time points are highlighted in Figure 3H. Transcriptional regulators were identified using the PlantTFCat tool. The absence of bubbles in certain modules is attributed to missing values (*e.g.* no genes with specific or amplified down-regulation under WD/S- were found in module M7, M10 and M16). D, Profiles of module eigengenes for modules significantly enriched for genes with a significant treatment effect (identified in C; means ± S.D, $n = 4$ replicates). Note that module M4 is not represented in A, because of the edge threshold cutoff used for the network visualization. E, Heatmap representing correlations (Spearman) between trait data (elements and osmotic potential) and module eigengenes. F, Boxplots showing the distribution by module of correlation (Spearman) coefficients for the comparison protein vs mRNA. Dots represent individual genes. Genes with a correlation > 0.5 (Protein vs mRNA) are highlighted in orange. Boundaries of the boxes represent the 25th and 75th percentiles, and horizontal lines within boxes represent medians.

selected and defined as treatment-driven modules (Figure 4D). Ten of these 12 modules were enriched for genes exhibiting a specific or amplified response under WD/S-, and were either up-regulated (M2, M6, M7, M9, M16) or down-regulated (M8, M20, M21, M25, M27) under this condition (Figure 4C). Hence, the selected treatment-driven modules are representative of the greater response induced by the stress combination, described above (Figure 3). In addition, some of these modules (M2, M4, M5, M6, M9, M25, M27) were also enriched for genes with a significant time × treatment interaction effect, and therefore constitute interesting targets for analyzing the influence of time on the stress response (Figure 4, C and D).

Correlations between modules and the accumulation of selected elements (C, N, S, N/S and C/N) and osmotic potential were then calculated (Figure 4E). This revealed that module M16 was highly correlated with these variables, particularly with S content (negatively), and the N/S ratio (positively, Figure 4E). Genes within M16 were highly expressed under both S- and WD/S-, as opposed to control and WD, across all time points (Figure 4D). Module M20 showed the opposite pattern of expression and therefore showed high correlation coefficients with the same variables (with opposite signs of correlation coefficients, Figure 4, D and E). We hypothesized that modules M16 and M20 are mainly driven by S availability and changes in the N/S ratio, independently of water availability. Nonetheless, the over-representation of genes with a specific or amplified response under WD/S- in both modules suggests that WD, when combined with S deficiency, also contributes to the variation in gene expression within these two modules (Figure 4D).

This co-expression network and the selected modules cover the main observations made with statistical analyses, while shedding light on the diversity of gene expression signatures in response to S deficiency with or without WD.

A module of response to S deficiency reveals known and putative new regulators of S-deficient conditions

To better dissect the responses induced by S-, applied alone or with WD, we focused on module M16, which grouped genes that were up-regulated in leaves in response to both S- and WD/S- (Figure 4D). A Gene Ontology (GO) enrichment analysis evidenced that several GO terms associated with sulfate assimilation and homeostasis, biosynthesis of S compounds (Met, Cys, glutathione), and processes related to redox homeostasis (*e.g.* ‘response to reactive oxygen species’, ‘ascorbate glutathione cycle’)

were significantly over-represented within M16 (Supplemental Figure S6; Supplemental Data Set S5). We also found that two sulfate transporters (SULTRs) were grouped into M16 and were up-regulated at most time points under both S- and WD/S- (*Psat2g074400* and *Psat3g185920*; Supplemental Figure S7). *Psat2g074400* is homologous to AtSULTR of group 1 involved in sulfate uptake and source to sink transport in Arabidopsis (Yoshimoto et al. 2002) and *Psat3g185920* is homologous to AtSULTR of group 4 involved in vacuolar sulfate efflux (Kataoka et al. 2004). This suggests that S deficiency (occurring alone or combined with WD) may activate the expression of genes involved in S transport and metabolism in leaves, possibly to ensure the production of S-containing antioxidant molecules like glutathione and to rebalance the availability of S and N.

Next, we selected genes with high module connectivity (module membership > 0.9) and strong negative correlation with S (gene significance for S < -0.9) within M16 (Figure 5A). In total, twenty-three genes were selected and designated as M16 hubs (Figure 5, A and B; Supplemental Data Set S7). Two M16 hubs corresponded to homologous genes of the OAS cluster gene *SULFUR DEFICIENCY INDUCED 1/2* (*SDI1/2; Psat3g142720* and *Psat3g144280*). We then looked for other members and found that all homologous genes of the Arabidopsis OAS cluster that were expressed in our experiment (nine in total) were highly induced under both S- and WD/S- and were grouped within module M16 (Supplemental Figure S8). Although only homologs of *SDI1/2* were identified as hubs using our criteria, seven of the nine homologs showed a module membership > 0.9 (Figure 5C). Interestingly, we also found that all of the ten genes encoding proteins that were up-regulated under S- and WD/S- in seeds in Henriet et al. (2021) were grouped in M16, with a high module membership (> 0.9, Figure 5C). Six of them are M16 hubs and include a thioredoxin (*Psat5g207000)* and a glutathione S-transferase (GST, *Psat6g125080*; Figure 5B). Together, these results highlight a potential conservation of the molecular responses to S deficiency between plant species (Arabidopsis and pea for the OAS cluster genes) and between tissues (leaves and seeds in pea), and demonstrates the robustness of our network analysis.

Module M16 was also the module with the highest overall correlation between mRNA and protein data (Figure 4F). In fact, the distribution of correlation coefficients (proteins vs mRNAs) within M16 was significantly different and higher (median = 0.672) as compared to other modules (median = 0.119; Supplemental Figure S9). This

458 corroborates the enrichment of processes associated with the biosynthesis of S-
459 containing molecules within the group of 308 genes with a Protein/mRNA correlation
460 greater than 0.5 (Figure 3I). In addition, we performed a co-expression network
461 analysis from proteomic data, using the same methodology as for transcriptomic data.
462 A network of nine modules was built, in which module MP1 was identified as a
463 treatment-driven module, correlated with both S content and the N/S ratio, and
464 exhibiting an accumulation profile similar to M16 (Supplemental Figure S10). This
465 module was enriched for pathways also revealed in M16, including S-related
466 processes (*e.g.* sulfate assimilation) and processes associated with redox
467 homeostasis (Supplemental Figure S11). Hence, the list of genes within module M16
468 greatly overlaps with the list of genes encoding the proteins found in module MP1
469 (Supplemental Figure S12). Such overlap was not observed for other modules of co-
470 expression (Supplemental Figure S12). To illustrate, a homologous gene of the OAS
471 cluster gene *APR3* (*Psat1g179680*) and four M16 hub genes showed similar profiles
472 between mRNAs and proteins, with an up-regulation under S- and WD/S- as compared
473 to control and WD (Supplemental Figures S8 and S13). Altogether, these results
474 suggest that genes within M16 may be more strongly regulated at the transcriptional
475 level and less subjected to post-transcriptional regulations, as compared to genes
476 found in other modules.

477 To identify potential regulators of genes grouped in module M16 – and in other
478 modules of co-expression – we searched for predicted regulatory connections between
479 transcription factors (TFs, regulators) and their target genes using a gene regulatory
480 network inference approach. To limit the number of predicted connections, both
481 regulators and targets were restricted to proteins or mRNAs that were significantly
482 affected by treatments (identified in Figure 3A). In total, this approach identified 6508
483 regulatory connections between 102 TFs and 4830 target genes (Supplemental Figure
484 S14; Supplemental Data Set S7). For module M16, 55 TFs were predicted to target
485 160 genes in total (Figure 5, D and E). A group of seven regulators have a higher
486 number of targets and are central to a regulatory module, composed of 21 of the 23
487 identified M16 hubs and of five orthologs of the Arabidopsis OAS cluster genes (Figure
488 5, D and E). The TF with the highest number of targets within M16 (45) corresponds to
489 a member of the MYB/SANT family (*Psat0s2726g0040*), and is predicted to regulate
490 all five OAS cluster genes found in this module (Figure 5, D and E; Supplemental Data
491 Set S7).

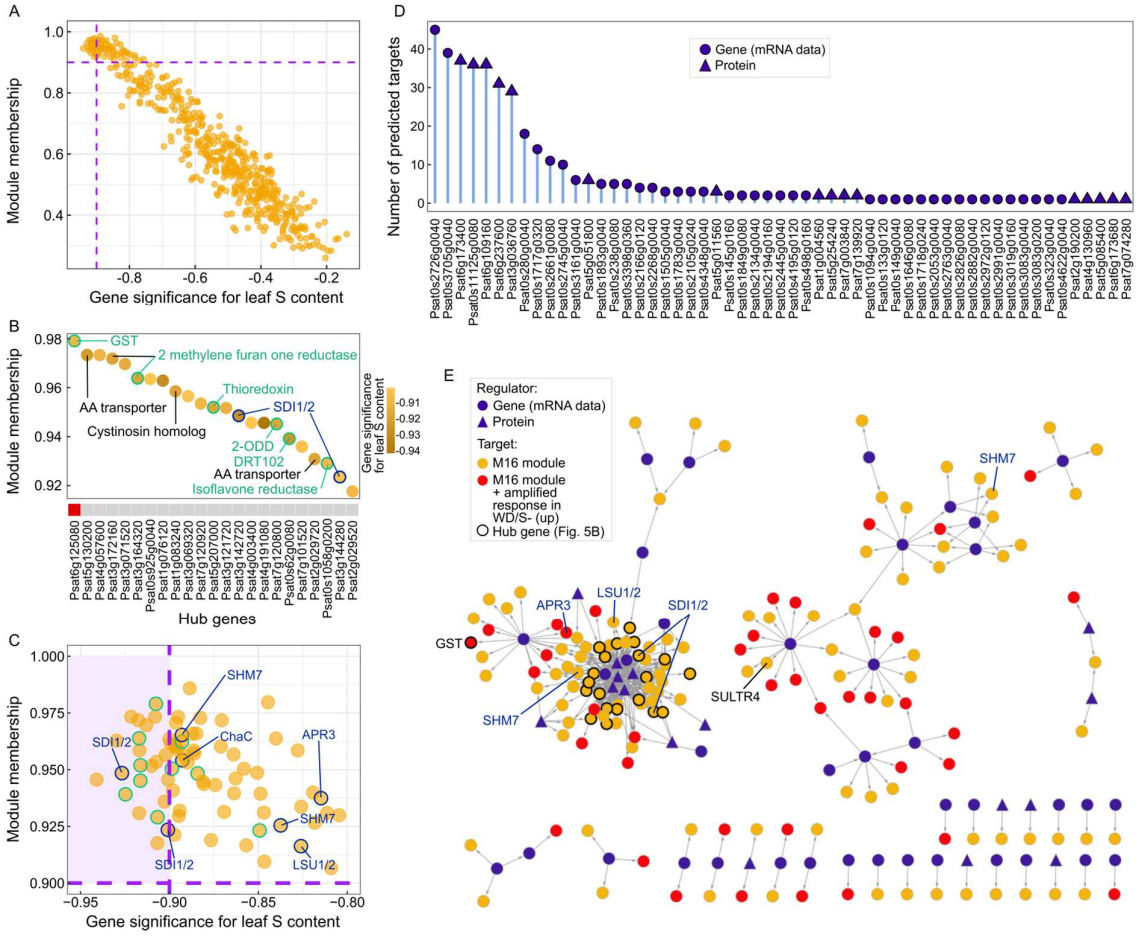

Figure 5. The M16 module reveals known and putative new regulators of response to sulfur deficiency (S-) combined or not with water deficit. A, Scatter plot of module membership vs gene significance for leaf S content in module M16. The horizontal and vertical purple dashed lines represent a module membership = 0.9 and a gene significance = -0.9, respectively. B, Dot plot ranking hub genes according to their module membership. Above gene IDs, red squares denote genes with amplified up-regulation under WD/S-, while grey squares represent genes without such amplified effect. C, Zoom of the scatter plot presented in A. The purple area delimits selected hub genes (gene significance < -0.9 and module membership > 0.9). In B and C, homologs of OAS cluster genes and genes encoding proteins that were up-regulated in pea seeds under S- and WD/S- in Henriet et al. (2021) are highlighted with black and green border lines, respectively. D, Predicted regulators of genes belonging to module M16. Regulators are TFs and correspond to proteins or mRNAs (when data for the TF was not available at the proteome level). Regulatory links were predicted using the method dynGENIE3. E, Regulatory network of M16 genes and their predicted regulators. Edges are oriented from regulators to target genes. M16 genes with an amplified up-regulation under WD/S- (identified in Figure 3F) are highlighted in red. AA, amino acid; GST, glutathione S-transferase; 2-ODD, bi-functional coumaroyl CoA and feruloyl CoA ortho-hydroxylase; DRT102, DNA damage repair toleration DRT.

Most of the M16 hubs were predicted to be targeted by multiple TFs and were found in the largest regulatory module (Figure 5E). Although most of them were strongly driven by S availability, independently of water availability, *Psat6g125080* – encoding a GST and identified as the M16 hub with the highest module membership (0.98, Figure 5B) – showed an amplified up-regulation under WD/S- (Figure 5C). Other

genes in M16 were specifically or more highly induced under WD/S- and include homologs of the OAS cluster genes *APR3* (*Psat4g006280*) and *ChaC* (*Psat6g042040*; Figure 5E; Supplemental Data Set S6). This suggests that stress combination amplified the core mechanisms of response to S deficiency.

Responses to stress combination are coordinated over time

We reasoned that genes exhibiting a specific or amplified up-regulation under WD/S- may correspond to genes important for the plant survival under this condition, which severely compromised plant growth (Figure 1). We selected three contrasted treatment-driven modules of co-expression, M2, M7 and M9, which were enriched for genes with a specific or amplified up-regulation under WD/S-, and with different kinetics of response (Figures 4D and 6A). Genes in M9 were specifically up-regulated at day 2 under WD/S-, as illustrated for hub genes within this module (Figure 6B). Genes in module M2 exhibited an amplified up-regulation in response to WD/S- (as compared to S-) at the end of the combined stress period (Figure 6, A and B). In addition, both M2 and M9 were enriched for genes with a significant time × treatment interaction effect (Figures 4C and 6B). These two modules can therefore be defined as time-specific modules of response to WD/S-. In contrast, genes in module M7 did not respond to WD/S- in a time-specific manner, and were up-regulated from day 2 to day 9 (Figure 6, A and B). Selected modules therefore showed unique gene expression signatures under stress combination, with early (M9, day 2), late (M2, day 9), or early to late (M7, day 2 to 9) responses (Figure 6A).

To identify biological pathways specifically activated early and/or lately under WD/S-, we compared enriched GO terms within modules M2, M7 and M9 (Supplemental Figure S15, Supplemental Data Set S5). First, this analysis revealed that genes up-regulated at multiple time points (module M7) play a role in responses to various stresses (*e.g.* heat, salt, UV, hypoxia, Supplemental Data Set S5), including the response to cadmium (Supplemental Figure S15). This suggests that module M7 corresponds to general stress-responsive genes, that may be activated under high stress intensity and that remain highly expressed if the stress continues. Second, we observed that M9 and M2 showed very specific GO enrichment results (Supplemental Figure S15). More specifically, module M9 is characterized by genes involved in signal transduction, protein phosphorylation, responses to oxidative stress and to hormones, as well as in the response to abiotic stress and in defense-related processes (Figure

549 6C; Supplemental Figure S15). On the other hand, module M2 is highly represented
550 by genes with a role in the regulation of chromatin accessibility and gene expression
551 (Figure 6C; Supplemental Figure S15). In addition, some epigenetic-related GO terms
552 like 'chromatin remodeling' and 'regulation of gene expression, epigenetic' are
553 specifically enriched in module M2, considering all modules of co-expression (M1 to
554 M27; Supplementary Figure S16). Taken together, these results suggest that cascades
555 of signalization are induced in leaves from the first two days following the beginning of
556 stress combination to turn on stress-responsive genes, some of which remaining
557 activated up to the recovery period, whereas changes in chromatin accessibility
558 operate after several days under high stress intensity.

559 We next asked whether modules M2 and M9, which showed very distinct timing of
560 response, were regulated by specific TFs or TF families. Using results of the gene
561 regulatory network inference (Supplemental Figure S14), we observed that some TF
562 families were predicted to preferentially regulate module M2 or M9. For instance, three
563 bZIP members were identified as putative regulators of modules M2, M7 and M9, with
564 most of their targets located in M9 (Figure 6C). Similarly, the NAM and Hap3/NF-YB
565 families were predicted to mainly regulate genes from module M2 (Figure 6C). One of
566 the bZIPs (*Psat0s3019g0160*), which we renamed R1, was predicted to target 56
567 (29%) M9 hubs, and was identified as the highest ranked regulator in terms of number
568 of predicted targets (overall, using all modules of co-expression, Supplemental Figure
569 S14). This gene is homologous to the Arabidopsis gene *SULPHATE UTILIZATION*
570 *EFFICIENCY 3* (*SUE3/VIP1, AT1G43700*). In Arabidopsis, the *sue3* mutant displayed
571 enhanced tolerance to sulfur deficiency and to heavy metals and oxidative stress (Wu
572 et al. 2010). In our data, this gene was induced under WD/S- at days 5 and 9 (Figure
573 6D), and may thus act as a repressor of module M9, which showed an early response
574 (day 2) to this stress condition. R1 is also predicted to regulate genes from module M2
575 (Figure 6C; Supplemental Data Set S7), which are related to changes in chromatin
576 accessibility and which showed similar expression profiles as R1. Thus, R1 could be a
577 positive regulator of M2 genes. In that connection, using DAP-Seq data published for
578 Arabidopsis (O'Malley et al. 2016) and GO information, we found that genes involved
579 in epigenetic regulation of gene expression and in various developmental processes
580 were over-represented within the set of genes identified as AtSUE3 targets
581 (Supplemental Figure S17).
582

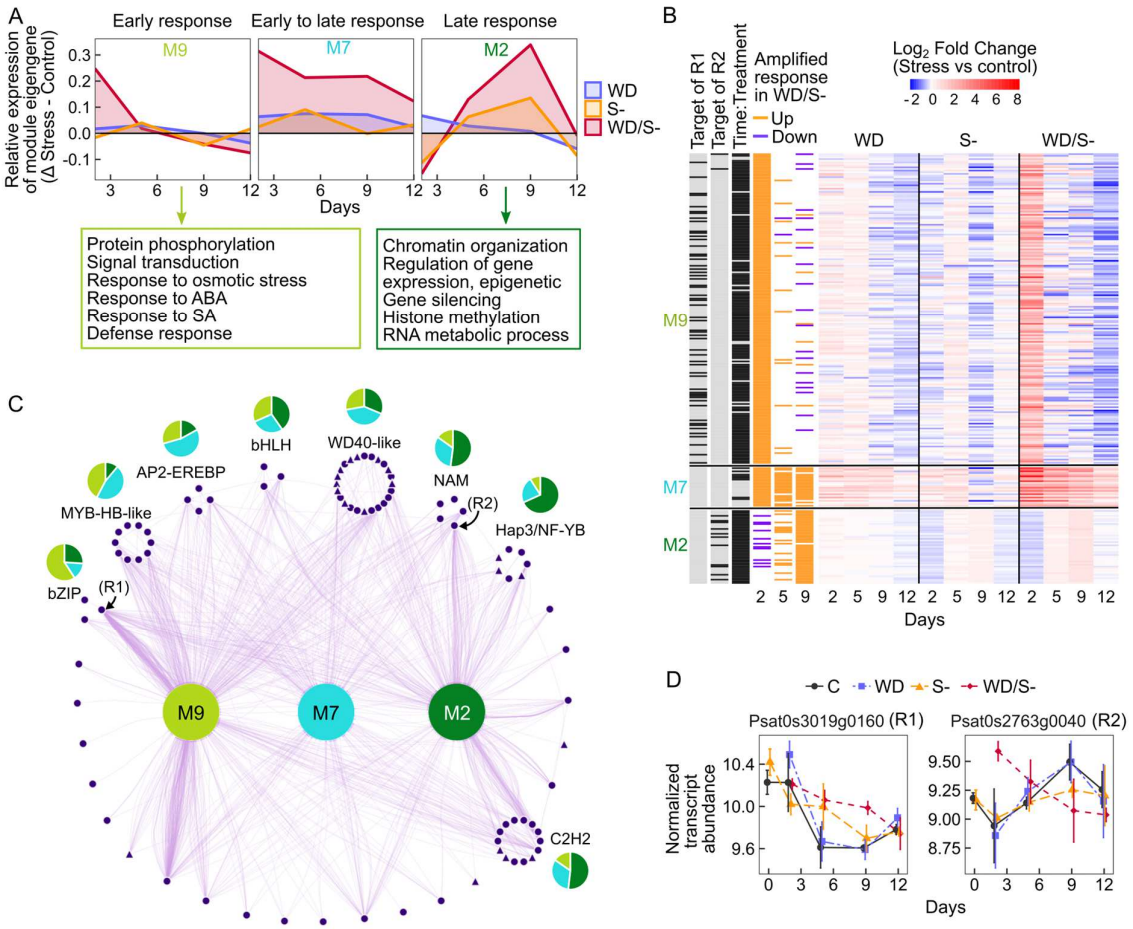

583

584 **Figure 6**. Modules of response to the stress combination show different timings of response. A, Area
585 charts representing the average changes in relative expression of module eigengenes under stress
586 conditions (Δ stress - control) for modules M9, M7 and M2. Below charts, selected enriched biological
587 processes within modules M9 and M2 are indicated. B, Heatmap of hubs (module membership > 0.9)
588 identified in modules M9, M7 and M2. The first three columns indicate whether (black) or not (grey)
589 genes were identified as targets of R1 and R2 (highlighted in D and E) and/or showed a significant time
590 × treatment interaction effect (Figure 3A). The next three columns highlight genes with a specific or
591 amplified response under WD/S- as compared to single stress conditions (identified in Figure 3E). The
592 last 12 columns represent changes in gene expression under stress as compared to control. Blue and
593 red colors indicate lower and higher values in the stress condition as compared to control, respectively.
594 C, Regulatory network of modules M9, M7 and M2 and their predicted regulators. Edges are oriented
595 from regulators to target genes. Regulators are grouped by TF family. For TF families with at least three
596 members, the proportion of modules M9, M7 and M2 within the predicted targets are represented as pie
597 charts. Regulators R1 and R2 shown on Figure 6D are highlighted. D, Gene expression profiles of TFs
598 R1 and R2 (means ± S.D, *n* = 4 biological replicates).

599

600 Most regulators were predicted to target genes from multiple modules. For
601 example, a NAM member referred to as R2 (*Psat0s2763g0040)* is predicted to regulate
602 hubs from both modules M2 and M9 (Figure 6, B and C). This gene is homologous to
603 the Arabidopsis gene *SUPPRESSOR OF GAMMA RESPONSE 1* (*SOG1*,
604 *AT1G25580*), a plant-specific transcriptional regulator that plays a major role in the

response to DNA damage (Preuss and Britt 2003; Yoshiyama et al. 2009). R2 was specifically up-regulated at day 2 under WD/S-, then at day 9 its expression was lower than under other three treatments. This regulator may therefore be a positive regulator of module M9 (early response to the combined stress) and a repressor of module M2 (late response).

Our results suggest that responses to stress combination are tightly coordinated over time, involving transcriptional regulators that may selectively activate and repress specific pathways in a time-specific manner.

Discussion

Stress combination can lead to unique molecular responses in plants, which could not be predicted from the effects observed under each individual stress. Here, we focused on the responses of pea to S- and WD, and investigated how the combination of stresses could accentuate the effects of single stresses or induce specific molecular signatures.

Overall, combination of stresses caused important modifications of the plant phenotype and leaf elemental composition, and of the leaf transcriptome and proteome. When occurring alone, WD had a moderate effect on the measured phenotypic variables, and fewer mRNAs and proteins were differentially accumulated in leaves under this condition as compared to other treatments (Figure 1 and 3). However, data collected at maturity on plants grown during the same experiment showed that the number of reproductive nodes and the one-seed weight were significantly reduced (Henriet et al. 2019). Hence, the plant responds to WD over the long term while still recovering. During stress imposition and after three days of rewatering, while WD had little effect when occurring alone, its strong impact when combined with S- evidenced a synergistic effect between the two stresses. The leaf osmotic potential at the end of the WD period (day 9, Figure 1) illustrates this synergistic effect, with a 20% decrease under WD/S-, whereas it was decreased by 4.2% and 9.3% under WD and S-, respectively. In leaves, highest contents of iron, zinc and cobalt were observed under the combined stress at days 9 and 12 (Figure 2, Supplemental Figure S2). While these elements are essential for plants, their hyperaccumulation can be detrimental to plant growth (Balafrej et al. 2020; Hu et al. 2021; Zahra et al. 2021). Similarly, leaf cadmium content was significantly higher at the end of the experiment under WD/S- as compared to other treatments

(Supplemental Figure S2). Higher accumulation of these elements under the combined stress could explain, at least in part, why the S-deficient plants did not survive an additional three days of WD (Henriet et al. 2019).

Our co-expression network analysis evidenced a module of genes (M2) with an amplified up-regulation under the combined stress at day 9, before plant rewatering, when stress intensity was the highest. This module was enriched for genes involved in chromatin organization and remodeling, as well as in epigenetic processes (Figure 6, Supplemental Figure S16). The activation of genes playing a role in the regulation of chromatin accessibility may reflect the activation of DNA damage responses (Casati and Gomez 2021). Our network analyses revealed R2 (*Psat0s2763g0040*) as a potential regulator of module M2, which is homolog to *SOG1* (*AT1G25580*), a plant-specific transcriptional regulator that plays a major role in the response to DNA damage (Preuss and Britt 2003; Yoshiyama et al. 2009). In pea leaves, *PsSOG1* was specifically induced in the early response to the combined stress (Figure 6). Under this condition that highly perturbed the plant development, we speculate that DNA damages may occur, possibly due to ROS burst, which would activate the DNA repair machinery through PsSOG1.

Single stresses have also caused alterations in the elemental composition of leaves. This suggests that the uptake and transport of elements have been disrupted by stress. Despite a drastic reduction in S contents in leaves under S-, either occurring alone or in combination with WD, we identified two pea SULTR genes belonging to module M16 that were highly up-regulated under S-limiting conditions (S- and WD/S-, Supplemental Figure S7). These two transporters belong to groups 1 (*Psat2g074400*) and 4 (*Psat3g185920*) implicated in sulfate uptake and efflux from the vacuole, respectively, and may play an important role to limit the impact of S- in leaves. The two S- conditions (S- and WD/S-) were also characterized by high molybdenum contents in leaves (Figure 2). The increased uptake and accumulation of molybdenum when S is limiting has been well documented in other crops (Shinmachi et al. 2010; Maillard et al. 2016). Sulfate and molybdenum having similar biochemical properties, molybdenum can be transported by sulfate transporters (Fitzpatrick et al. 2008). Of the three molybdate transporters annotated in pea and expressed in our experiment, two were grouped in the co-expression module M22 (*Psat5g026520* and *Psat6g031280*) and did not respond to stress, and one (*Psat4g172720*) was grouped in the module M20 and was down-regulated under S- and WD/S-. The increased content of

673 molybdenum in leaves under S- conditions could therefore result from an increased
674 transport by the two SULTR mentioned above. Similar results were observed in
675 *Brassica napus*, where S- induced higher molybdenum contents in leaves and strong
676 up-regulation of SULTR of group 1 in roots, whereas molybdate transporters showed
677 slight up-regulation or no differential expression (Maillard et al. 2016). Likewise, the
678 increased concentrations of toxic elements such as cadmium in pea leaves may result
679 from the activation of transporters of essential or beneficial nutrients (Zhao et al.
680 2022b). For instance, cadmium entry can be mediated by Mn transporters NRAMPs
681 (Cailliatte et al. 2010; Ishimaru et al. 2012; Sasaki et al. 2012) and by the Fe transporter
682 IRT1 (Vert et al. 2021).

683 While most DEGs were observed under S- and WD/S- conditions, suggesting a
684 high contribution of S availability to changes in gene expression, our analyses enabled
685 us to differentiate between genes primarily regulated by S availability and those
686 exhibiting specific or amplified responses to the combined stress. All expressed pea
687 homologs of the Arabidopsis OAS cluster were highly up-regulated under both S- and
688 WD/S-, with an up-regulation detected from day 0 (*i.e.* before WD imposition),
689 suggesting that their regulation by S deficiency is independent of water availability
690 (Figure 5, Supplemental Figure S8). However, orthologs of *APR3* (*Psat4g006280*) and
691 *ChaC* (*Psat6g042040*) showed an amplified up-regulation under stress combination as
692 compared to S deficiency applied alone (Figure 5; Supplemental Data Set S6). For
693 these genes, S availability may not be the only factor influencing their transcription.
694 Previous studies have shown that OAS cluster genes not only respond to S deprivation,
695 but also to other stresses where OAS accumulates, including conditions that generate
696 reactive oxygen species (ROS, Apodiakou and Hoefgen, 2023). Although ROS are by-
697 products of several metabolic processes, they accumulate under stress and can induce
698 oxidative stress, causing cellular damages. GO terms associated with responses to
699 ROS and redox homeostasis were enriched in both modules of response to S
700 deficiency (M16) and in modules of response to the combined stress (M7 and M9,
701 Supplemental Data Set S5). Analysis of module M16 revealed two hub genes encoding
702 enzymes with antioxidant roles, a GST (*Psat6g125080*) and a thioredoxin
703 (*Psat5g207000*), which showed similar patterns of response to stress at both mRNA
704 and protein levels (Figure 5, Supplemental Figures S12 and S13). Interestingly, these
705 two proteins were evidenced in pea seeds, in a cluster of antioxidant proteins that were
706 up-regulated in response to S- occurring alone or in combination with WD (Henriet et

al. 2021; Bonnot et al. 2023). This suggests that accumulation of ROS probably occurred in both pea leaves and seeds of the treated pea plants, which activated responses to oxidative stress involving similar key players between leaves and seeds. Moreover, in leaves, the GST showed an amplified up-regulation under the combined stress as compared to S deficiency applied alone (Figure 5), as also observed for *PsAPR3* and *PsChaC* (mentioned above). We speculate that these three genes may respond to stress intensity, which was higher under stress combination, whereas other OAS cluster genes and other M16 hubs may rather respond to S availability.

Despite known connections between S assimilation and redox homeostasis processes (reviewed in Bonnot et al., 2023), the extent to which these pathways share similar regulatory mechanisms remains unclear. Using a gene regulatory network approach, we identified a member of the MYB TF family, *Psat0s2726g0040*, which was predicted to control the expression of most of the M16 hubs, several orthologs of the Arabidopsis OAS cluster genes and genes with a role in the maintenance of the redox balance (Figure 5; Supplemental Data Set S7). Recently, several TFs were proposed to regulate an extended OAS cluster co-expression gene network in Arabidopsis, using the Plant Regulomics database (Ran et al. 2020; Apodiakou and Hoefgen 2023). These TFs included *AT3G10580*, a MYB related family member, that we found in the same orthogroup as *Psat0s2726g0040* (Supplemental Table S1). This gene may therefore represent an interesting candidate regulator of OAS cluster genes in plants and, as suggested by our results in pea, of genes involved in redox homeostasis.

Among other interesting candidate regulators identified in our gene regulatory network analysis, the gene R1, which is homolog to *SUE3/VIP1* (*AT1G43700)*, was predicted to regulate a high number of genes (Figure 6). Our results suggested that it may act as a repressor of genes activated in the early response to the combined stress condition and involved in signaling and response to osmotic stress (module M9), and as an activator of several genes with a late response and participating in the regulation of chromatin accessibility (module M2). In Arabidopsis, SUE3/VIP1 was shown to bind to the promoter of stress-responsive genes, activating their transcription, including genes *TRXH8* (*AT1G69880*) and *MYB44* (Pitzschke et al. 2009). Thioredoxins-h type (TRXH) are enzymes having an antioxidant function that are commonly induced in plants in response to diverse stresses including drought and osmotic stress (Schürmann and Jacquot 2000; Zhang et al. 2011; Chibani et al. 2021). Under drought stress, MYB44 accumulates in Arabidopsis and participates in the increased

741 acetylation of H3K27 in stress-responsive genes, activating their transcription (Zhao et
742 al. 2022a). These previous findings support the hypothetical role of Ps-SUE3/VIP1 in
743 leaves, where it could play a pivotal role in the coordination of early vs late responses
744 to high stress intensity induced by multi-stress conditions.
745 We anticipate that our results pave the way for reverse genetic analyses of
746 selected candidate regulators, which may help modifying the plant capacity to induce
747 molecular responses to abiotic stresses under S-deprived conditions, in efforts to
748 improve crop tolerance to stress.
749

750 **Materials and methods**

751 **Plant growth, treatments and samplings**

752 Pea plants (*Pisum sativum* L., 'Caméor' genotype) were obtained from the experiment
753 described in (Henriet et al. 2019). Briefly, germinated seeds were sown in pots filled
754 with a mixture of perlite and sand (3/1, v/v). Plants were grown in a greenhouse, at
755 19°C/15°C (day/night) with a 16 h/8 h (light/dark) photoperiod. Plants were irrigated
756 with a nitrate- and S-rich (S+) solution containing 0.3 mM $MgSO_4 \cdot 7\ H_2O$ as a source
757 of S (Henriet et al., 2019). After three weeks (5/6 node stage), S- treatment was applied
758 to half of the plants: the substrate was rinsed twice using deionized water and twice
759 using a S- nutritive solution depleted of $MgSO_4 \cdot 7\ H_2O$ but containing 1.16 mM $MgCl_2$,
760 then plants were watered using this solution until the end of the experiment. After eight
761 days following the beginning of S- treatment, all plants (including S+ plants) at the 8-
762 node stage (on the primary branch, secondary branches were removed across the
763 experiment) were moved to an automated Plant Phenotyping Platform for Plant and
764 Micro-organism Interactions (4PMI, Dijon, France). Plants were weighted and watered
765 four times a day to maintain a water-holding capacity of the substrate of 100%. At
766 flowering of the second/third flowering nodes (*i.e.*, 16 days after the onset of S
767 deficiency), half of the plants (half of the S+ and half of the S deficiency-treated plants)
768 were subjected to WD: irrigation was stopped to reach a water-holding capacity of the
769 substrate of 50%, then this value was maintained for nine days. This level of irrigation
770 corresponded to a leaf water potential of -1.3 MPa (Henriet et al., 2019). After nine
771 days, plants were rewatered normally, with their respective nutritive solution (S+ or S-
772). This experimental setup allowed to get four different sets of plants, grown under:
773 control (no stress applied) condition, S-, WD, or a combination of S- and WD.
774

775 **Sampling and phenotypic and physiological measurements**

776 Sampling and measurements were performed on days 0, 2, 5, 9 and 12 after the start
777 of the WD application. Note that day 12 corresponds to three days after the end of WD,
778 *i.e.* three days of re-watering for the WD and WD/S conditions. A total of eigth plants
779 per condition and time point were grown and used for all experiments described below.

780 For leaf area measurements, the leaves of each individual plant were spread out
781 and scanned with an EPSON GT20000 (model J151A) scanner, and leaf area was
782 measured using a custom image processing algorithm. Dry weight measurements
783 were performed after drying tissues at 80°C for 48 h.

784 For osmotic potential estimation, leaflets from the last fully expanded leaves of
785 two independent plants were collected, placed in a syringe, frozen in liquid nitrogen
786 and stored at –80°C. After thawing, the cell sap was pressed out of a syringe, collected
787 and centrifuged at 10,000 × g for 10 min at 4°C. The osmolality of the corresponding
788 supernatant was measured using a vapour pressure osmometer (Wescor model 5520,
789 Bioblock Scientific, Illkirch, France), and the osmotic potential (MPa) was then
790 calculated according to the Van't Hoff equation: $\pi=(-R\times T\times$osmolality of the extract),
791 where T is the absolute temperature and R is the constant of perfect gas.

792 For -omics analyses, leaves were collected from the first two reproductive nodes
793 of two independent plants and pooled, resulting in four replicates. Samples were snap-
794 frozen in liquid nitrogen and stored at -80°C. The same samples were used for
795 transcriptomics, proteomics, ionomics and SCN content determination (see below).

796

797 **Element analyses**

798 S, C and N contents were determined from dried ground leaf samples (four biological
799 replicates) using the Dumas method (Allen et al. 1974). Contents of C and N were
800 determined from 5 mg of tissue powder on a Flash 2000 Elemental Analyzer (Thermo
801 Fisher Scientific), and contents of S were determined from 20 mg of tissue powder
802 mixed with 5 mg of tungsten trioxide on an elemental PYRO cube analyzer
803 (Elementar). Two technical replicates per biological replicate were performed.

804 Elements referred to as 'Ionomics data' in the manuscript correspond to essential
805 macro-nutrients (phosphorus, potassium, calcium, magnesium), micro-nutrients (iron,
806 boron, manganese, zinc, copper, molybdenum, nickel) and other elements (cobalt,
807 cadmium, lead, arsenic, vanadium), quantified by HR ICP-MS (Thermo Scientific,
808 Element 2TM). For each sample, 40 mg of dried ground leaf material were

resuspended in 800 µL of concentrated HNO_3, 200 µL H_2O_2 and 1 mL of Milli-Q water. All samples were then spiked with three internal standard solutions containing gallium, rhodium and iridium with final concentrations of 5, 1 and 1 µg L^{-1}, respectively. After microwave acidic digestion (Multiwave ECO, Anton Paar, les Ulis, France), all samples were diluted with 50 mL of Milli-Q water to obtain solutions containing 2.0% (v/v) nitric acid. Before HR ICP-MS analysis, samples were filtered through a 0.45 µm teflon filtration system (Digifilter, SCP Science, Courtaboeuf, France). Quantification of each element was performed using external standard calibration curves and concentrations were expressed in µg.g^{-1} of leaves.

Shotgun proteomics

Protein sample preparation, analysis by LC-MS/MS and quantification, were performed as described in (Henriet et al. 2021). Briefly, total proteins were extracted from 110 mg of ground leaf tissues. Protein samples were lyophilized, then solubilized in buffer containing 6 M urea, 2 M thiourea, 10 mM DTT, 30 mM Tris-HCl pH 8.8 and 0.1% zwitterionic acid labile surfactant. For each sample, 20 µg of proteins were alkyled then digested overnight at 37°C using trypsin. Trypsin-digested proteins were desalted and analyzed by LC-MS/ MS using an Eksigent nlc425 device coupled to a Q Exactive mass spectrometer (ThermoFisher Scientific), with a glass needle (non-coated capillary silica tips, 360/20-10, New Objective). Proteins were identified using X!Tandem v.2015.04.01.1 (Craig and Beavis 2004), by matching peptides against the *P. sativum* v.1a database (https:// urgi.versailles.inra.fr/jbrowse/gmod_jbrowse/; (Kreplak et al. 2019). Identified proteins were filtered and grouped using the X!TandemPipeline software v.3.4.3 (Langella et al. 2017). Relative protein quantification was performed using the MassChroQ software v.2.2 (Valot et al. 2011). Protein quantification data is provided in Supplemental Data Set S3.

RNA extraction and sequencing

Extraction of RNAs from leaf tissues, RNA-sequencing (RNA-Seq) and data processing were performed as described in (Henriet et al. 2019). Briefly, total RNAs were extracted from ground leaf tissues using an RNeasy Plant Mini Kit (QIAGEN), then a DNAse treatment with an RNase-Free DNase Set (QIAGEN) and a purification step using lithium chloride precipitation were performed. RNA quality was checked on a 2100 Bioanalyzer (Agilent Genomics). RNA-Seq libraries were prepared using an

Illumina TruSeq Stranded mRNA sample prep kit, and 11 PCR cycles were performed to amplify the libraries. Library quality was checked using a Fragment Analyzer (Agilent Genomics) and libraries were sequenced on the Illumina HiSeq3000 to obtain 2×150 bp paired-end reads. Quality of raw reads was assessed using the FastQC v0.11.2 software (https://www.bioinformatics.babraham.ac.uk/projects/fastqc/). Trimming of low-quality and adapter sequences was performed on raw reads using Trimmomatic v0.32 (Bolger et al. 2014). Trimmed reads with less than 25 bp and unpaired reads were removed. Filtered reads were mapped to the *P. sativum* v1a reference genome (https://urgi.versailles.inra.fr/Species/Pisum/Pea-Genome-project), using the alignment program HISAT2 v2.0.5 (Kim et al. 2015). Read counting was performed using FeatureCounts v1.5.0-p3 (Liao et al. 2014) on gene annotation v1b (Henriet et al. 2019). Only genes with at least 10 reads total in the experiment were considered as expressed and were used for downstream analyses (29575 genes in total). Gene expression was normalized using the VST transformation proposed by the DESeq2 package (Love et al. 2014). Gene expression data is provided in Supplemental Dataset S3.

Statistical analyses

Identification of variables significantly affected by treatments

All statistical analyses were performed with the software program R v. 4.1.2 (R Core Team 2022). To assess the influence of S deficiency at the beginning of the experiment on phenotypic variables, on leaf CNS contents, and on the leaf osmotic potential, unpaired Student's t-tests were performed to compare treatments S- and control at day 0. Significant difference between treatments was judged at P-value < 0.05.

For data collected from days 2 to 9, the effects of time, treatments and the interaction between these main effects were analyzed using the following model: design = ~ Time + Treatment + Time:Treatment. For transcriptomics, differential expression analysis was performed from raw counts of the 29575 filtered genes that were considered as expressed (see above). Likelihood ratio tests (LRTs) were performed with the DESeq2 package (Love et al. 2014), using the model described above. The LRT is conceptually similar to an analysis of variance (ANOVA) calculation in linear regression (Love et al. 2014). For other -omics data, two-way ANOVAs were performed for each individual variable using the aov() function. For all data, significance of factors was judged at $P < 0.05$ after FDR correction using the

Benjamini–Hochberg procedure (Benjamini and Hochberg 1995). Comparisons of treatments were then performed at each time point. For transcriptomics, pairwise comparisons were realized using the DESeq2 package (Love et al. 2014). For other -omics data, Tukey's honestly significant difference (HSD) mean- separation tests were performed, using the TukeyHSD() function. Variables were considered as differentially responding to treatments at a given time point (*e.g.* in response to S- as compared to control at day 2) if they showed *i*) a significant treatment effect (FDR < 0.05, LRTs or ANOVAs) and *ii*) a significant difference between treatments (FDR < 0.05, pairwise comparisons for transcriptomics; adjusted P-value < 0.05, Tukey's HSD tests for other -omics data). To consider as significant both variables with high or low magnitude of change in response to stress, no cutoff was applied on Fold Change values.

For data obtained at day 12, the same procedure was employed as for the analysis at days 2-9, with the following modification in the model used for LRTs (transcriptomics) and ANOVAs (other -omics data): design = ~ Treatment. Statistical results are provided in Supplemental Dataset S2.

Enrichment analyses

Gene Ontology (GO) enrichment analyses were conducted using the TopGO R package v. 2.46.0 (Alexa and Rahnenfuhrer 2022), with the Elim method and Fisher's exact tests. GO terms with a *P*-value < 0.01 were considered as significantly enriched in the selected subset of genes. Results are provided in Supplemental Data Set S5. The GO term enrichment analysis performed from Arabidopsis genes was computed using the interface of The Arabidopsis Information Resource for GO enrichment analyses for plants (https://www.arabidopsis.org/tools/ go_term_enrichment.jsp), powered by the Panther classification system (Mi et al. 2019). Significantly enriched GO terms were considered at FDR < 0.05 (Fisher's exact tests).

To identify the enrichment of specific sets of genes (with a time, treatment or time:treatment effects, with an amplified response under the combined stress condition, or transcriptional regulators) within network modules, Fisher's exact tests were performed. Proportions of these specific sets of genes within each module were compared to their proportions in all genes found in the network. Significant differences were judged at $P < 0.05$. Results are provided in Supplemental Data Set S9.

Correlation between proteomics and transcriptomics data

For each expressed gene for which a protein was successfully quantified in shotgun proteomics (2240 genes in total), correlations were calculated between protein and mRNA data, with the R cor() function and the Spearman method. Two separate analyses were performed: one using data obtained from all treatment conditions (Figure 3G), and one that was conducted by treatment (Figure 3H). Correlation coefficients are provided in Supplemental Data Set S6.

Network analyses

Co-expression network

Weighted Gene Co-expression Network Analyses were conducted with the R package 'WGCNA' v. 1.72-5 (Langfelder and Horvath 2008). Two separate analyses were performed, from data obtained at the 1) transcriptome and 2) proteome levels. Prior to analysis, transcriptomic data were filtered to remove genes with low expression values that could introduce noise into the network analysis. Genes with raw counts > 10 in at least 50% of the samples were considered for the analysis, which represents 21281 genes. Normalized genes expression values (after VST transformation) were then used. No filtering was applied on proteomic data, all 2261 quantified proteins were used for the analysis. Data obtained at days 0 (control and S- conditions), 2, 5, 9 and 12 were used. Adjacency matrices were built using a soft threshold power of 12 and 16 for the analyses performed from transcriptomic and proteomic data, respectively. To identify modules of co-expression, the minimum module size was set at 30. Similar modules were merged, using a dissimilarity threshold of 0.25. Module eigengene values were used to represent module expression patterns. Module information is provided in Supplemental Data Set S7. To identify pea transcriptional regulators, PlantTFcat was run on proteins of the v1b pea genome annotation, using default parameters (Jin et al. 2017). Results are provided in Supplemental Data Set S8. For selected pea genes, homologous genes in Arabidopsis were identified using reciprocal BLASTP search (https://plants.ensembl.org/Multi/Tools/Blast). The phylogeny of sulfate transporters (SULTRs) was built from protein sequences, using the interactive phylogenetics module of the Dicots PLAZA v5 database (https://bioinformatics.psb.ugent.be/plaza/versions/plaza_v5_dicots/). The software MUSCLE v. 3.8.31 and FastTree v. 2.1.7 were used for the multiple sequence alignment and the phylogenetic tree, respectively.

Gene regulatory network

Regulatory connections between transcription factors and target genes were predicted using the dynamical Gene Network Inference with Ensemble of trees (dynGENIE3) method (Huynh-Thu and Geurts 2018). Genes with low expression values were filtered out prior to analysis, as described above for the co-expression network analysis. In addition, this analysis was restricted to genes that showed a significant treatment effect (Figure 3A). Transcriptional regulators that were annotated as “transcription factors” (PlantTFcat analysis, Supplemental Data Set S6) were selected as input. For these input genes, data obtained at the protein level were preferred, when available, otherwise transcriptomic data were used. Transcriptomic data were used for the set of target genes. In total, 1172 input genes – which included 40 proteins – and 14180 potential target genes were used for this analysis. Regulatory links with a weight > 0.01 were selected to build regulatory networks. Results are provided in Supplemental Data Set S7. Arabidopsis homologs of selected candidate regulators were identified using the Dicots PLAZA v5 database (https://bioinformatics.psb.ugent.be/plaza/versions/plaza_v5_dicots/).

Data visualization

Heatmaps were generated with the R package ‘pheatmap’ v. 1.0.12 (Kolde 2019). Venn diagrams were drawn using the R package ‘eulerr’ v. 7.0.1 (Larsson 2022). Enriched GO terms were represented as described in (Bonnot et al. 2019). Networks were visualized with the software ‘CYTOSCAPE’ v. 3.9.0 (Smoot et al. 2011), using a Prefuse Force Directed Layout. For co-expression networks (generated with WGCNA), links with a weight > 0.15 (transcriptome analysis) or a weight > 0.10 (proteome analysis) were used for visualization. All other plots were prepared using the R package ‘ggplot2’ v. 3.4.4 (Wickham 2016).

Data availability

Raw mass spectrometry files have been deposited to the ProteomeXchange Consortium via the PRIDE partner repository with the dataset identifier PXD048279. Raw RNA-Seq data (fasta files and read counting data) are accessible from the Gene Expression Omnibus (GEO) database, www.ncbi.nlm.nih.gov/geo, with the identifier GSE252351. All other data are available as Supplemental Data Sets.

Supplemental data

Supplemental Table S1. Arabidopsis genes identified in the same orthogroup (ORTHO05D000330) as *Psat0s2726g0040*, according to the Dicots PLAZA v.5 database.

Supplemental Figure S1. Quantification of sulfur (S) in leaves: correlation between the two quantification methods.

Supplemental Figure S2. Accumulation profiles of elements over time in leaves.

Supplemental Figure S3. Volcano plots representing statistical significance versus magnitude of change for mRNAs.

Supplemental Figure S4. Selected enriched biological processes in the list of genes with a specific or amplified down-regulation under WD/S- as compared to single stress conditions.

Supplemental Figure S5. Profiles of module eigengenes for modules identified in the co-expression network analysis, performed from transcriptomic data.

Supplemental Figure S6. Enriched biological processes in the list of 520 genes grouped in module M16.

Supplemental Figure S7. Response to stress of sulfate transporters.

Supplemental Figure S8. Response to stress of OAS cluster genes.

Supplemental Figure S9. Distribution of correlation (Protein vs mRNA) coefficients within M16 and other modules.

Supplemental Figure S10. Co-accumulation network of proteins reveals modules with distinct patterns of response to stress.

Supplemental Figure S11. Enriched biological processes in the list of 333 proteins grouped in module MP1.

Supplemental Figure S12. Overlap between co-expression modules (transcriptomics data) and co-accumulation modules (proteomics data).

Supplemental Figure S13. Expression profiles (mRNAs and proteins) of selected hubs in module M16.

Supplemental Figure S14. Prediction of regulatory connections between TFs and their target genes.

Supplemental Figure S15. Selected enriched biological processes in modules M2, M7 and M9.

Supplemental Figure S16. Enrichment of biological processes related to epigenetic mechanisms in co-expression modules.

Supplemental Figure S17. Enriched biological processes within the list of genes targeted by AT1G43700, identified as homologous to the regulator R1.

Supplemental Data Set S1. Quantification results (Phenomics, osmotic potential, elements).

Supplemental Data Set S2. Statistical results.

Supplemental Data Set S3. Transcriptomics and proteomics data.

Supplemental Data Set S4. Correlations between proteins and mRNAs.

Supplemental Data Set S5. Gene Ontology enrichment analysis.

Supplemental Data Set S6. Genes with an amplified response under WD/S- as compared to single stress conditions.

Supplemental Data Set S7. Network results.

Supplemental Data Set S8. Transcription factors in *Pisum sativum.*

Supplemental Data Set S9. Enrichment of gene sets within modules.

Acknowledgments

We thank the members of the 4PMI Platform (Phenotyping Platform for Plant and Plant Microorganisms Interactions, INRAE, Dijon) for their excellent technical support during plant growth and all members of the FILEAS team for helping with sample collection and measurements of plants phenotypic variables. We also thank Mickaël Lamboeuf for the development of the custom image processing algorithm used for the calculation of the leaf surface area, Sylvie Girodet for CN measurements and the GISMO platform (Université de Bourgogne Franche-Comté, Dijon, France) for S measurements; Rémy-Félix Serre from the GeT-PlaGe core facility (Castanet-Tolosan, France) for the sequencing of mRNAs and pre-processing of the mRNA-Seq data. We also thank Marion Prudent for her help with the experimental setup, and Christine Le Signor for helpful discussions to interpret the data.

Funding

The PhD grant of CH was funded by the French Ministry for Higher Education and Research. Analyses were supported by the European Union (FP7 Program ‘LEGATO’, project n°613551, greenhouse experiments); by the INRAE Plant Breeding department

(project PRORESO, proteomics) and by the TIMAC Agro International - Groupe Roullier within the framework of the FUI-SERAPIS project (RNA-Seq).

Conflict of interest statement: The authors declare no competing interests.

References

Aarabi F, Kusajima M, Tohge T, Konishi T, Gigolashvili T, Takamune M, Sasazaki Y, Watanabe M, Nakashita H, Fernie AR, et al. Sulfur deficiency-induced repressor proteins optimize glucosinolate biosynthesis in plants. Science Advances. 2016:**2**(10):e1601087–e1601087. https://doi.org/10.1126/sciadv.1601087

Aarabi F, Rakpenthai A, Barahimipour R, Gorka M, Alseekh S, Zhang Y, Salem MA, Brückner F, Omranian N, Watanabe M, et al. Sulfur deficiency-induced genes affect seed protein accumulation and composition under sulfate deprivation. Plant Physiology. 2021:**187**(4):2419–2434. https://doi.org/10.1093/plphys/kiab386

Alexa A and Rahnenfuhrer J. topGO: Enrichment analysis for Gene Ontology. 2022.

Allen WM, Berrett S, and Patterson DSP. A biochemical study of experimental Johne's disease. Journal of Comparative Pathology. 1974:**84**(3):385–389. https://doi.org/10.1016/0021-9975(74)90013-9

Apodiakou A and Hoefgen R. New insights into the regulation of plant metabolism by O -acetylserine: sulfate and beyond. Journal of Experimental Botany. 2023:**74**(11):3361–3378. https://doi.org/10.1093/jxb/erad124

Azodi CB, Lloyd JP, and Shiu S-H. The cis-regulatory codes of response to combined heat and drought stress in Arabidopsis thaliana. NAR Genomics and Bioinformatics. 2020:**2**(3):1–16. https://doi.org/10.1093/nargab/lqaa049

Balafrej H, Bogusz D, Triqui Z-EA, Guedira A, Bendaou N, Smouni A, and Fahr M. Zinc Hyperaccumulation in Plants: A Review. Plants. 2020:**9**(5):562. https://doi.org/10.3390/plants9050562

Benjamini Y and Hochberg Y. Controlling the false discovery rate: a practical and powerful approach to multiple testing. Journal of the Royal Statistical Society Series B (Methodological). 1995:**57**:289–300. https://doi.org/10.2307/2346101

Bolger AM, Lohse M, and Usadel B. Trimmomatic: a flexible trimmer for Illumina sequence data. Bioinformatics. 2014:**30**(15):2114–2120. https://doi.org/10.1093/bioinformatics/btu170

Bonnot T, Bachelet F, Boudet J, Le Signor C, Bancel E, Vernoud V, Ravel C, and Gallardo K. Sulfur in determining seed protein composition: present understanding of its interaction with abiotic stresses and future directions. Journal of Experimental Botany. 2023:**74**(11):3276–3285. https://doi.org/10.1093/jxb/erad098

Bonnot T, Gillard M, and Nagel D. A Simple Protocol for Informative Visualization of Enriched Gene Ontology Terms. Bio-101. 2019:e3429. https://doi.org/10.21769/BioProtoc.3429

Bonnot T, Martre P, Hatte V, Dardevet M, Leroy P, Bénard C, Falagán N, Martin-Magniette M-L, Deborde C, Moing A, et al. Omics Data Reveal Putative Regulators of Einkorn Grain Protein Composition under Sulfur Deficiency. Plant Physiology. 2020:**183**(2):501–516. https://doi.org/10.1104/pp.19.00842

Borja Reis AF de, Rosso LHM, Davidson D, Kovács P, Purcell LC, Below FE, Casteel SN, Knott C, Kandel H, Naeve SL, et al. Sulfur fertilization in soybean: A meta-analysis on yield and seed composition. European Journal of Agronomy. 2021:**127**:126285. https://doi.org/10.1016/j.eja.2021.126285

Cailliatte R, Schikora A, Briat J-F, Mari S, and Curie C. High-Affinity Manganese Uptake by the Metal Transporter NRAMP1 Is Essential for Arabidopsis Growth in Low Manganese Conditions. The Plant Cell. 2010:**22**(3):904–917. https://doi.org/10.1105/tpc.109.073023

Casati P and Gomez MS. Chromatin dynamics during DNA damage and repair in plants: new roles for old players. Journal of Experimental Botany. 2021:**72**(11):4119–4131. https://doi.org/10.1093/jxb/eraa551

Chibani K, Pucker B, Dietz K, and Cavanagh A. Genome-wide analysis and transcriptional regulation of the typical and atypical thioredoxins in Arabidopsis thaliana. FEBS Letters. 2021:**595**(21):2715–2730. https://doi.org/10.1002/1873-3468.14197

Cohen I, Zandalinas SI, Huck C, Fritschi FB, and Mittler R. Meta-analysis of drought and heat stress combination impact on crop yield and yield components. Physiologia Plantarum. 2021:**171**(1):66–76. https://doi.org/10.1111/ppl.13203

Connolly EL and Guerinot ML. Iron stress in plants. Genome Biology. 2002:**3**(8):1–4. https://doi.org/10.1186/gb-2002-3-8-reviews1024

Craig R and Beavis RC. TANDEM: matching proteins with tandem mass spectra. Bioinformatics. 2004:**20**(9):1466–1467. https://doi.org/10.1093/bioinformatics/bth092

Detzel A, Krüger M, Busch M, Blanco-Gutiérrez I, Varela C, Manners R, Bez J, and Zannini E. Life cycle assessment of animal-based foods and plant-based protein-rich alternatives: an environmental perspective. Journal of the Science of Food and Agriculture. 2022:**102**(12):5098–5110. https://doi.org/10.1002/jsfa.11417

Fitzpatrick KL, Tyerman SD, and Kaiser BN. Molybdate transport through the plant sulfate transporter SHST1. FEBS Letters. 2008:**582**(10):1508–1513. https://doi.org/10.1016/j.febslet.2008.03.045

Haneklaus S, Bloem E, and Schnug E. History of Sulfur Deficiency in Crops. . In. Sulfur: A Missing Link between Soils, Crops, and Nutrition. (John Wiley & Sons, Ltd), pp. 45-58–6. https://doi.org/10.2134/agronmonogr50.c4

Henriet C, Aimé D, Térézol M, Kilandamoko A, Rossin N, Combes-Soia L, Labas V, Serre R-F, Prudent M, Kreplak J, et al. Water stress combined with sulfur deficiency in pea affects yield components but mitigates the effect of deficiency on seed globulin composition. Journal of Experimental Botany. 2019:**70**(16):4287–4304. https://doi.org/10.1093/jxb/erz114

Henriet C, Balliau T, Aimé D, Le Signor C, Kreplak J, Zivy M, Gallardo K, and Vernoud V. Proteomics of developing pea seeds reveals a complex antioxidant network underlying the response to sulfur deficiency and water stress. Journal of Experimental Botany. 2021:**72**(7):2611–2626. https://doi.org/10.1093/jxb/eraa571

Hu X, Wei X, Ling J, and Chen J. Cobalt: An Essential Micronutrient for Plant Growth? Frontiers in Plant Science. 2021:**12**(November):1–24. https://doi.org/10.3389/fpls.2021.768523

Hubberten H-M, Klie S, Caldana C, Degenkolbe T, Willmitzer L, and Hoefgen R. Additional role of O-acetylserine as a sulfur status-independent regulator during plant growth. The Plant Journal. 2012:**70**(4):666–677. https://doi.org/10.1111/j.1365-313X.2012.04905.x

Huynh-Thu VA and Geurts P. dynGENIE3: dynamical GENIE3 for the inference of gene networks from time series expression data. Scientific Reports. 2018:**8**(1):3384. https://doi.org/10.1038/s41598-018-21715-0

IPCC. IPCC, 2023: Climate Change 2023: Synthesis Report. A Report of the Intergovernmental Panel on Climate Change. Contribution of Working Groups I, II and III to the Sixth Assessment Report of the Intergovernmental Panel on Climate Change (Geneva, Switzerland).

Ishimaru Y, Takahashi R, Bashir K, Shimo H, Senoura T, Sugimoto K, Ono K, Yano M, Ishikawa S, Arao T, et al. Characterizing the role of rice NRAMP5 in Manganese, Iron and Cadmium Transport. Scientific Reports. 2012:**2**(1):286. https://doi.org/10.1038/srep00286

Jacques C, Forest M, Durey V, Salon C, Ourry A, and Prudent M. Transient Nutrient Deficiencies in Pea: Consequences on Nutrient Uptake, Remobilization, and Seed Quality. Frontiers in Plant Science. 2021:**12**(December):1–14. https://doi.org/10.3389/fpls.2021.785221

Jin J, Tian F, Yang D-C, Meng Y-Q, Kong L, Luo J, and Gao G. PlantTFDB 4.0: toward a central hub for transcription factors and regulatory interactions in plants. Nucleic Acids Research. 2017:**45**(D1):D1040–D1045. https://doi.org/10.1093/nar/gkw982

Kataoka T, Watanabe-Takahashi A, Hayashi N, Ohnishi M, Mimura T, Buchner P, Hawkesford MJ, Yamaya T, and Takahashi H. Vacuolar Sulfate Transporters Are Essential Determinants Controlling Internal Distribution of Sulfate in Arabidopsis. Plant Cell. 2004:**16**(10):2693–2704. https://doi.org/10.1105/tpc.104.023960

Kim D, Langmead B, and Salzberg SL. HISAT: a fast spliced aligner with low memory requirements. Nature Methods. 2015:**12**(4):357–360. https://doi.org/10.1038/nmeth.3317

Kolde R. pheatmap: Pretty Heatmaps. 2019.

Kreplak J, Madoui M-A, Cápal P, Novák P, Labadie K, Aubert G, Bayer PE, Gali KK, Syme RA, Main D, et al. A reference genome for pea provides insight into legume genome evolution. Nature Genetics. 2019:**51**(9):1411–1422. https://doi.org/10.1038/s41588-019-0480-1

Langella O, Valot B, Balliau T, Blein-Nicolas M, Bonhomme L, and Zivy M. X!TandemPipeline: A Tool to Manage Sequence Redundancy for Protein

Inference and Phosphosite Identification. Journal of Proteome Research. 2017:**16**(2):494–503. https://doi.org/10.1021/acs.jproteome.6b00632

Langfelder P and Horvath S. WGCNA: an R package for weighted correlation network analysis. BMC Bioinformatics. 2008:**9**(1):559. https://doi.org/10.1186/1471-2105-9-559

Larsson J. eulerr: Area-Proportional Euler and Venn Diagrams with Ellipses. 2022.

Lecomte C, Richer V, Gauffreteau A, Jeuffroy MH, Bouviala M, Brun C, Buridan C, Klein A, Lantoine FX, Marchand D, et al. Combining a multi-environment trial and a diagnosis method to assess potential yield and main limiting factors of three highly different pea types. European Journal of Agronomy. 2023:**146**(April). https://doi.org/10.1016/j.eja.2023.126823

Liao Y, Smyth GK, and Shi W. featureCounts: an efficient general purpose program for assigning sequence reads to genomic features. Bioinformatics. 2014:**30**(7):923–930. https://doi.org/10.1093/bioinformatics/btt656

Love MI, Huber W, and Anders S. Moderated estimation of fold change and dispersion for RNA-seq data with DESeq2. Genome Biology. 2014:**15**(12):550. https://doi.org/10.1186/s13059-014-0550-8

Mahalingam R, Duhan N, Kaundal R, Smertenko A, Nazarov T, and Bregitzer P. Heat and drought induced transcriptomic changes in barley varieties with contrasting stress response phenotypes. Frontiers in Plant Science. 2022:**13**(December):1–24. https://doi.org/10.3389/fpls.2022.1066421

Maillard A, Etienne P, Diquélou S, Trouverie J, Billard V, Yvin J-C, and Ourry A. Nutrient deficiencies modify the ionomic composition of plant tissues: a focus on cross-talk between molybdenum and other nutrients in Brassica napus. Journal of Experimental Botany. 2016:**67**(19):5631–5641. https://doi.org/10.1093/jxb/erw322

Mi H, Muruganujan A, Ebert D, Huang X, and Thomas PD. PANTHER version 14: more genomes, a new PANTHER GO-slim and improvements in enrichment analysis tools. Nucleic Acids Research. 2019:**47**(D1):D419–D426. https://doi.org/10.1093/nar/gky1038

Mittler R. Abiotic stress, the field environment and stress combination. Trends in Plant Science. 2006:**11**(1):15–19. https://doi.org/10.1016/j.tplants.2005.11.002

Mondal S, Pramanik K, Panda D, Dutta D, Karmakar S, and Bose B. Sulfur in Seeds: An Overview. Plants. 2022:**11**(3):450. https://doi.org/10.3390/plants11030450

O'Malley RC, Huang SC, Song L, Lewsey MG, Bartlett A, Nery JR, Galli M, Gallavotti A, and Ecker JR. Cistrome and epicistrome features shape the regulatory DNA landscape. Cell. 2016:**165**(5):1280–1292. https://doi.org/10.1016/j.cell.2016.04.038

Paine RT, Tegner MJ, and Johnson E a. Ecological Surprises. Ecosystems. 1998:**1**(July):535–545.

Pitzschke A, Djamei A, Teige M, and Hirt H. VIP1 response elements mediate mitogen-activated protein kinase 3-induced stress gene expression. Proceedings of the National Academy of Sciences. 2009:**106**(43):18414–18419. https://doi.org/10.1073/pnas.0905599106

Poisson E, Trouverie J, Brunel-Muguet S, Akmouche Y, Pontet C, Pinochet X, and Avice J-C. Seed Yield Components and Seed Quality of Oilseed Rape Are Impacted by Sulfur Fertilization and Its Interactions With Nitrogen Fertilization. Frontiers in Plant Science. 2019:**10**. https://doi.org/10.3389/fpls.2019.00458

Poore J and Nemecek T. Reducing food's environmental impacts through producers and consumers. Science. 2018:**360**(6392):987–992. https://doi.org/10.1126/science.aaq0216

Preuss SB and Britt AB. A DNA-Damage-Induced Cell Cycle Checkpoint in Arabidopsis. Genetics. 2003:**164**(1):323–334. https://doi.org/10.1093/genetics/164.1.323

R Core Team. R: A Language and environment for statistical computing. 2022.

Ran X, Zhao F, Wang Y, Liu J, Zhuang Y, Ye L, Qi M, Cheng J, and Zhang Y. Plant Regulomics: a data-driven interface for retrieving upstream regulators from plant multi-omics data. The Plant Journal. 2020:**101**(1):237–248. https://doi.org/10.1111/tpj.14526

Rasmussen S, Barah P, Suarez-Rodriguez MC, Bressendorff S, Friis P, Costantino P, Bones AM, Nielsen HB, and Mundy J. Transcriptome responses to combinations of stresses in *Arabidopsis*. Plant Physiology. 2013:**161**(4):1783–1794. https://doi.org/10.1104/pp.112.210773

Ristova D and Kopriva S. Sulfur signaling and starvation response in Arabidopsis. iScience. 2022:**25**(5):104242. https://doi.org/10.1016/j.isci.2022.104242

Rizhsky L, Liang H, and Mittler R. The Combined Effect of Drought Stress and Heat Shock on Gene Expression in Tobacco. Plant Physiology. 2002:**130**(3):1143–1151. https://doi.org/10.1104/pp.006858

Rizhsky L, Liang H, Shuman J, Shulaev V, Davletova S, and Mittler R. When defense pathways collide. The response of arabidopsis to a combination of drought and heat stress 1[w]. Plant Physiology. 2004:**134**(4):1683–1696. https://doi.org/10.1104/pp.103.033431

Samanta S, Singh A, and Roychoudhury A. Involvement of Sulfur in the Regulation of Abiotic Stress Tolerance in Plants. . In. Protective Chemical Agents in the Amelioration of Plant Abiotic Stress. (Wiley), pp. 437–466. https://doi.org/10.1002/9781119552154.ch22

Sasaki A, Yamaji N, Yokosho K, and Ma JF. Nramp5 Is a Major Transporter Responsible for Manganese and Cadmium Uptake in Rice. The Plant Cell. 2012:**24**(5):2155–2167. https://doi.org/10.1105/tpc.112.096925

Scherer HW. Sulphur in crop production. European Journal of Agronomy. 2001:**14**(2):81–111. https://doi.org/10.1016/S1161-0301(00)00082-4

Schürmann P and Jacquot J-P. PLANT THIOREDOXIN SYSTEMS REVISITED. Annual Review of Plant Physiology and Plant Molecular Biology. 2000:**51**(1):371–400. https://doi.org/10.1146/annurev.arplant.51.1.371

Shinmachi F, Buchner P, Stroud JL, Parmar S, Zhao F-J, McGrath SP, and Hawkesford MJ. Influence of Sulfur Deficiency on the Expression of Specific Sulfate Transporters and the Distribution of Sulfur, Selenium, and Molybdenum in Wheat. Plant Physiology. 2010:**153**(1):327–336. https://doi.org/10.1104/pp.110.153759

Smoot ME, Ono K, Ruscheinski J, Wang P-L, and Ideker T. Cytoscape 2.8: new features for data integration and network visualization. Bioinformatics. 2011:**27**(3):431–432. https://doi.org/10.1093/bioinformatics/btq675

Stagnari F, Maggio A, Galieni A, and Pisante M. Multiple benefits of legumes for agriculture sustainability: an overview. Chemical and Biological Technologies in Agriculture. 2017:**4**(1):2. https://doi.org/10.1186/s40538-016-0085-1

Tan JW, Shinde H, Tesfamicael K, Hu Y, Fruzangohar M, Tricker P, Baumann U, Edwards EJ, and Rodríguez López CM. Global transcriptome and gene co-expression network analyses reveal regulatory and non-additive effects of

drought and heat stress in grapevine. Frontiers in Plant Science. 2023:**14**(February):1–15. https://doi.org/10.3389/fpls.2023.1096225

Valot B, Langella O, Nano E, and Zivy M. MassChroQ: A versatile tool for mass spectrometry quantification. PROTEOMICS. 2011:**11**(17):3572–3577. https://doi.org/10.1002/pmic.201100120

Varshney RK, Pandey MK, Bohra A, Singh VK, Thudi M, and Saxena RK. Toward the sequence-based breeding in legumes in the post-genome sequencing era. Theoretical and Applied Genetics. 2019:**132**(3):797–816. https://doi.org/10.1007/s00122-018-3252-x

Vert G, Grotz N, Dédaldéchamp F, Gaymard F, Guerinot ML, Briat JF, and Curie C. CORRECTION: IRT1, an arabidopsis transporter essential for iron uptake from the soil and for plant growth. The Plant Cell. 2021:**33**(2):439–440. https://doi.org/10.1093/plcell/koaa033

Wickham H. ggplot2: Elegant Graphics for Data Analysis. 2016.

Wu Y, Zhao Q, Gao L, Yu X-M, Fang P, Oliver DJ, and Xiang C-B. Isolation and characterization of low-sulphur-tolerant mutants of Arabidopsis. Journal of Experimental Botany. 2010:**61**(12):3407–3422. https://doi.org/10.1093/jxb/erq161

Yoshimoto N, Takahashi H, Smith FW, Yamaya T, and Saito K. Two distinct high-affinity sulfate transporters with different inducibilities mediate uptake of sulfate in *Arabidopsis* roots. The Plant Journal. 2002:**29**(4):465–473. https://doi.org/10.1046/j.0960-7412.2001.01231.x

Yoshiyama K, Conklin PA, Huefner ND, and Britt AB. Suppressor of gamma response 1 (SOG1) encodes a putative transcription factor governing multiple responses to DNA damage. Proceedings of the National Academy of Sciences. 2009:**106**(31):12843–12848. https://doi.org/10.1073/pnas.0810304106

Zahra N, Hafeez MB, Shaukat K, Wahid A, and Hasanuzzaman M. Fe toxicity in plants: Impacts and remediation. Physiologia Plantarum. 2021:**173**(1):ppl.13361. https://doi.org/10.1111/ppl.13361

Zandalinas SI and Mittler R. Plant responses to multifactorial stress combination. New Phytologist. 2022:**234**(4):1161–1167. https://doi.org/10.1111/nph.18087

Zandalinas SI, Sengupta S, Fritschi FB, Azad RK, Nechushtai R, and Mittler R. The impact of multifactorial stress combination on plant growth and survival. New Phytologist. 2021:**230**(3):1034–1048. https://doi.org/10.1111/nph.17232

Zhang C-J, Zhao B-C, Ge W-N, Zhang Y-F, Song Y, Sun D-Y, and Guo Y. An Apoplastic H-Type Thioredoxin Is Involved in the Stress Response through Regulation of the Apoplastic Reactive Oxygen Species in Rice. Plant Physiology. 2011:**157**(4):1884–1899. https://doi.org/10.1104/pp.111.182808

Zhao B, Shao Z, Wang L, Zhang F, Chakravarty D, Zong W, Dong J, Song L, and Qiao H. MYB44-ENAP1/2 restricts HDT4 to regulate drought tolerance in Arabidopsis. PLOS Genetics. 2022a:**18**(11):e1010473. https://doi.org/10.1371/journal.pgen.1010473

Zhao F-J, Tang Z, Song J-J, Huang X-Y, and Wang P. Toxic metals and metalloids: Uptake, transport, detoxification, phytoremediation, and crop improvement for safer food. Molecular Plant. 2022b:**15**(1):27–44. https://doi.org/10.1016/j.molp.2021.09.016

Author contributions

Research design: CH, VV and KG; Data acquisition: CH, DA, T Balliau, AO and MZ; Data processing: T Bonnot, CH, MT and JK; Data mining and visualization: T Bonnot; Data interpretation: T Bonnot, CH, MT, VV and KG; Writing – original draft: T Bonnot, CH, VV and KG; Manuscript review and editing: T Bonnot, CH, DA, JK, MT, T Bailliau, AO, MZ, VV and KG.

Supplemental Table S1. Arabidopsis genes identified in the same orthogroup (ORTHO05D000330) as *Psat0s2726g0040*, according to the Dicots PLAZA v.5 database.

Gene ID	Description
AT1G49010	MYB-like transcription factor; ATMYBL, MYBS1
AT2G38090	Duplicated homeodomain-like superfamily protein
AT3G10580	Homeodomain-like superfamily protein
AT3G10585	Homeodomain-like superfamily protein
AT3G11280	Putative transcription factors interacting with the gene product of VHA-B1
AT4G09450	Duplicated homeodomain-like superfamily protein
AT5G01200	Duplicated homeodomain-like superfamily protein
AT5G04760	R-R-type MYB protein; DIV2, DIVARICATA2
AT5G05790	Duplicated homeodomain-like superfamily protein
AT5G08520	Duplicated homeodomain-like superfamily protein; MYBS2
AT5G58900	R-R-type MYB protein ; DIV1, DIVARICATA1

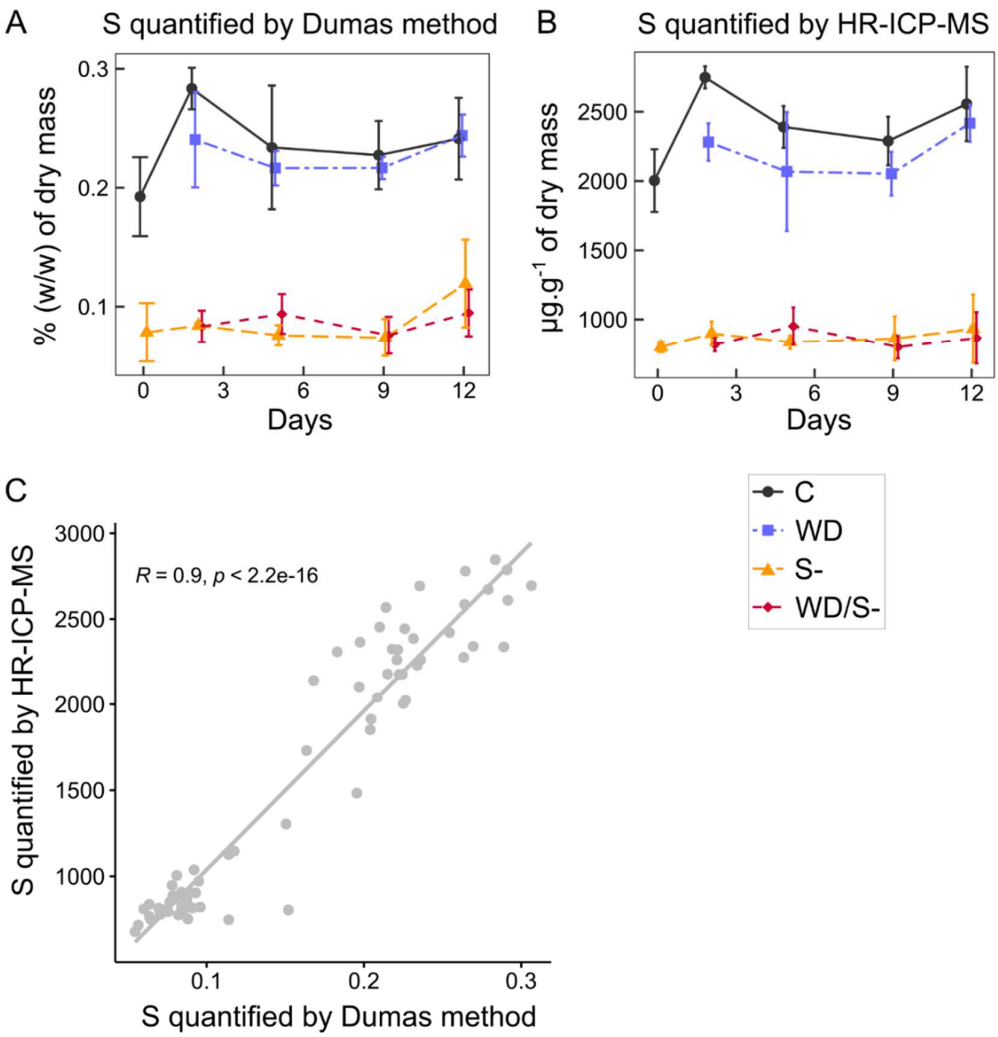

Supplemental Figure S1. Quantification of sulfur (S) in leaves: correlation between the two quantification methods. A, S percent measured using the Dumas method. B, S measured using high-resolution inductively coupled plasma mass spectrometry (HR ICP-MS). In A and B, data are means ± S.D of $n = 4$ replicates. C: control, WD: water deficit, S-: S deficiency. Note that day 12 corresponds to three days of rewatering in the WD and WD/S- conditions. C, Correlation between data obtained by HR ICP-MS (ionomics, B) and by the Dumas method (A). The correlation (Spearman) coefficient and P-value are indicated.

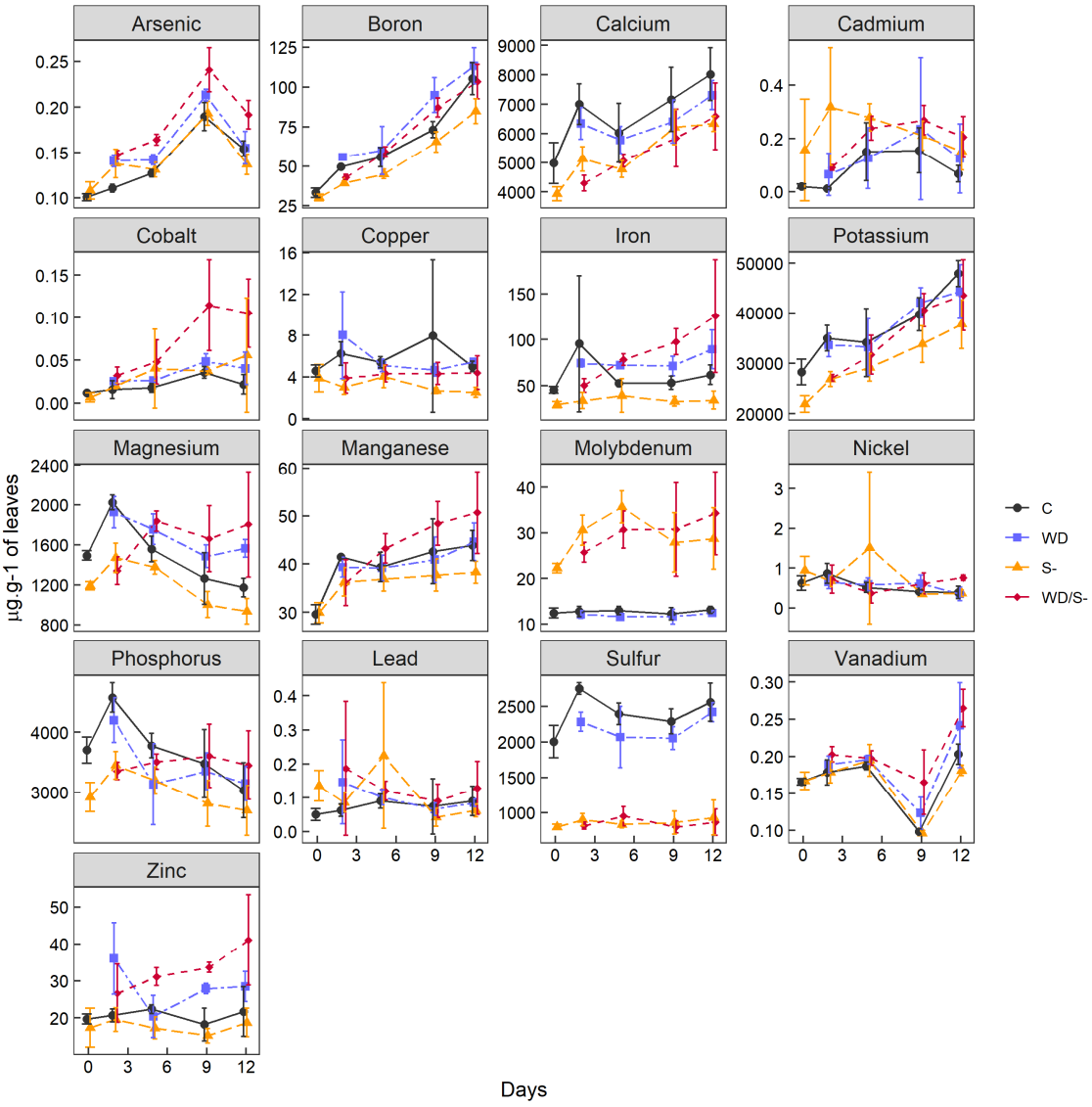

1343

1344 **Supplemental Figure S2**. Accumulation profiles of elements over time in leaves. Data
1345 are means ± S.D of *n* = 4 biological replicates. C: control, WD: water deficit, S-: Sulfur
1346 deficiency. Note that day 12 corresponds to three days of rewatering in the WD and
1347 WD/S- conditions.

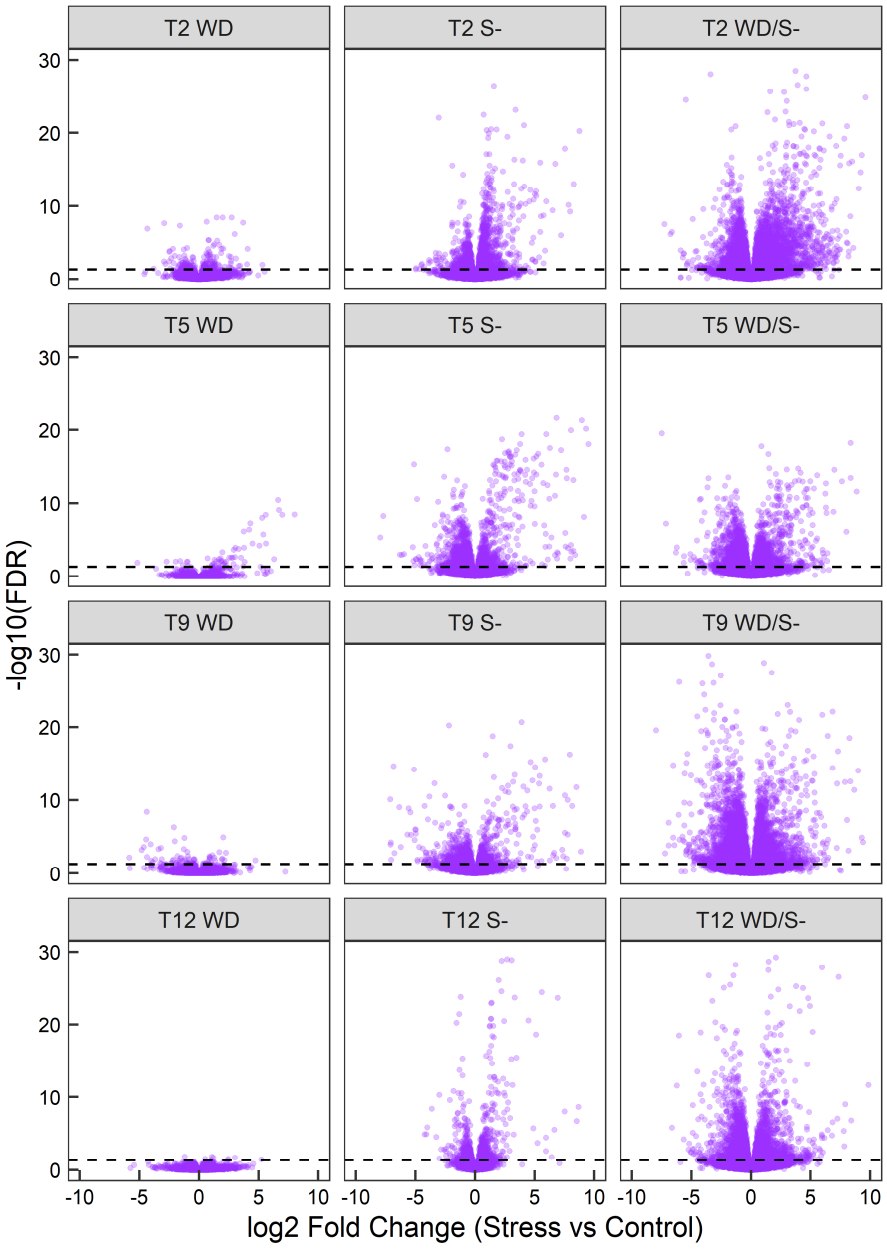

Supplemental Figure S3. Volcano plots representing statistical significance (-log10[FDR]) versus magnitude of change (Log_2 Fold Change) for mRNAs. WD: water deficit, S-: Sulfur deficiency. Note that T12 corresponds to three days of rewatering in the WD and WD/S- conditions.

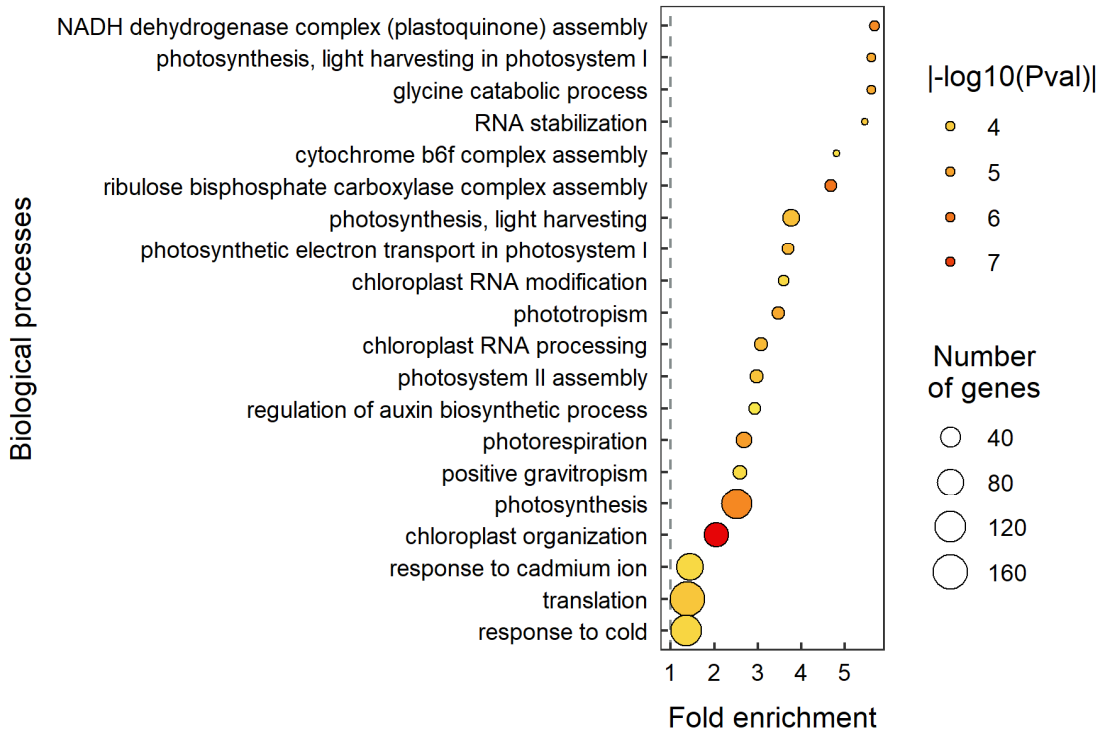

1353

1354 **Supplemental Figure S4**. Selected enriched biological processes in the list of genes
1355 with a specific or amplified down-regulation under WD/S- as compared to single stress
1356 conditions. The top 20 enriched GO terms (based on P-values) are represented.
1357 Results of the GO enrichment analysis are provided in Supplemental Data Set S5.

1358

1359

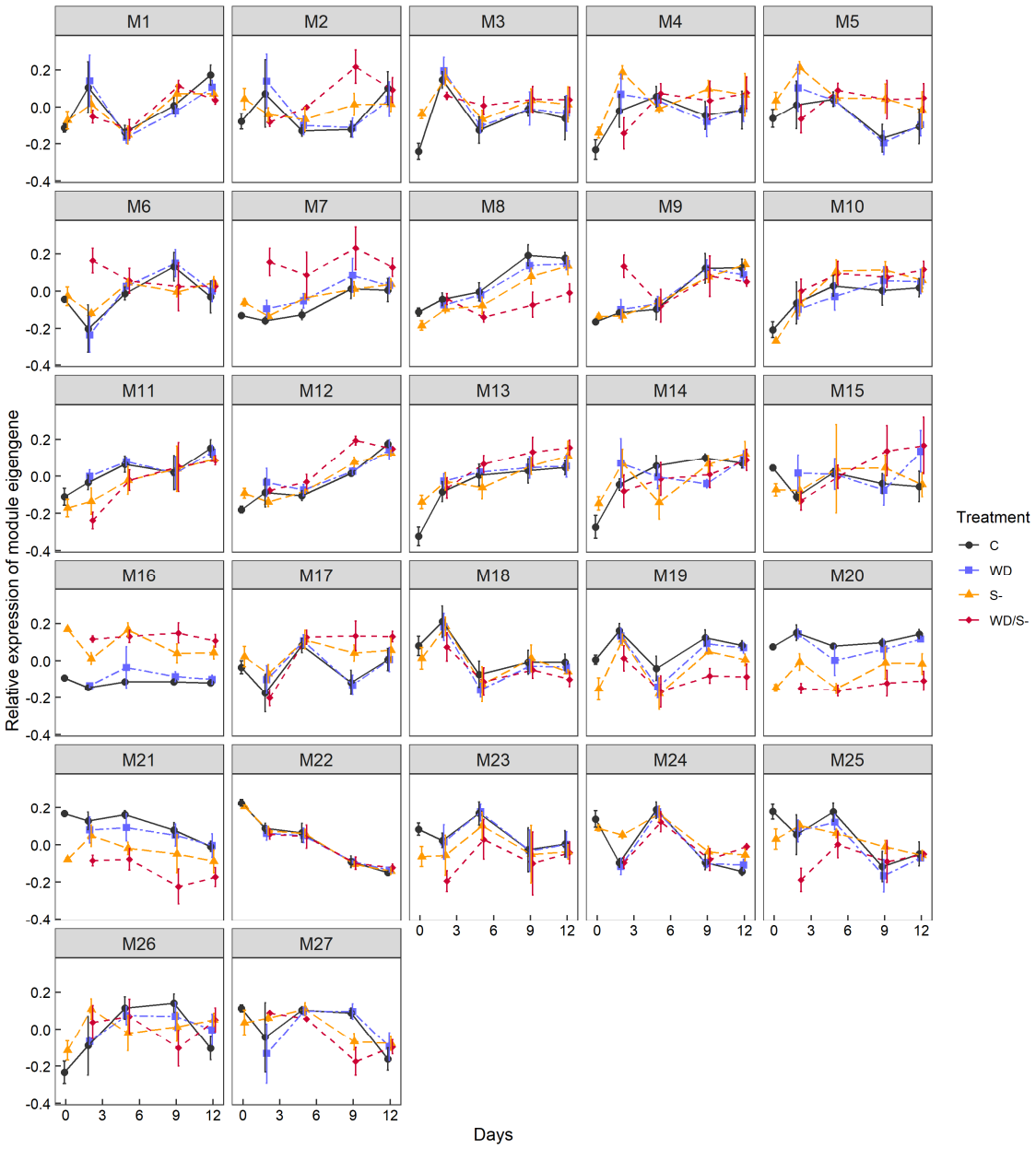

Supplemental Figure S5. Profiles of module eigengenes for modules identified in the co-expression network analysis, performed from transcriptomic data. Data are means ± S.D. for $n = 4$ replicates. C: control, WD: water deficit, S-: Sulfur deficiency. Note that day 12 corresponds to three days of rewatering in the WD and WD/S- conditions.

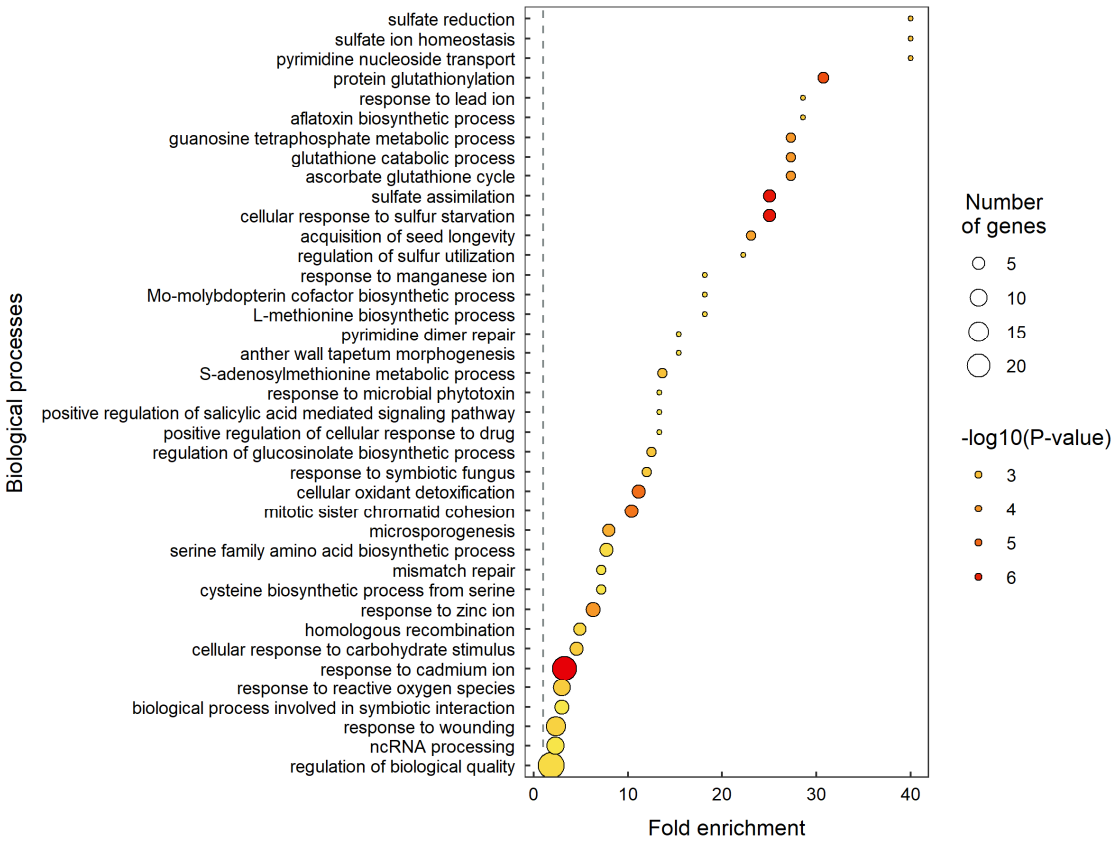

Supplemental Figure S6. Enriched biological processes in the list of 520 genes grouped in module M16. Results of the GO enrichment analysis for all modules are provided in Supplemental Data Set S5.

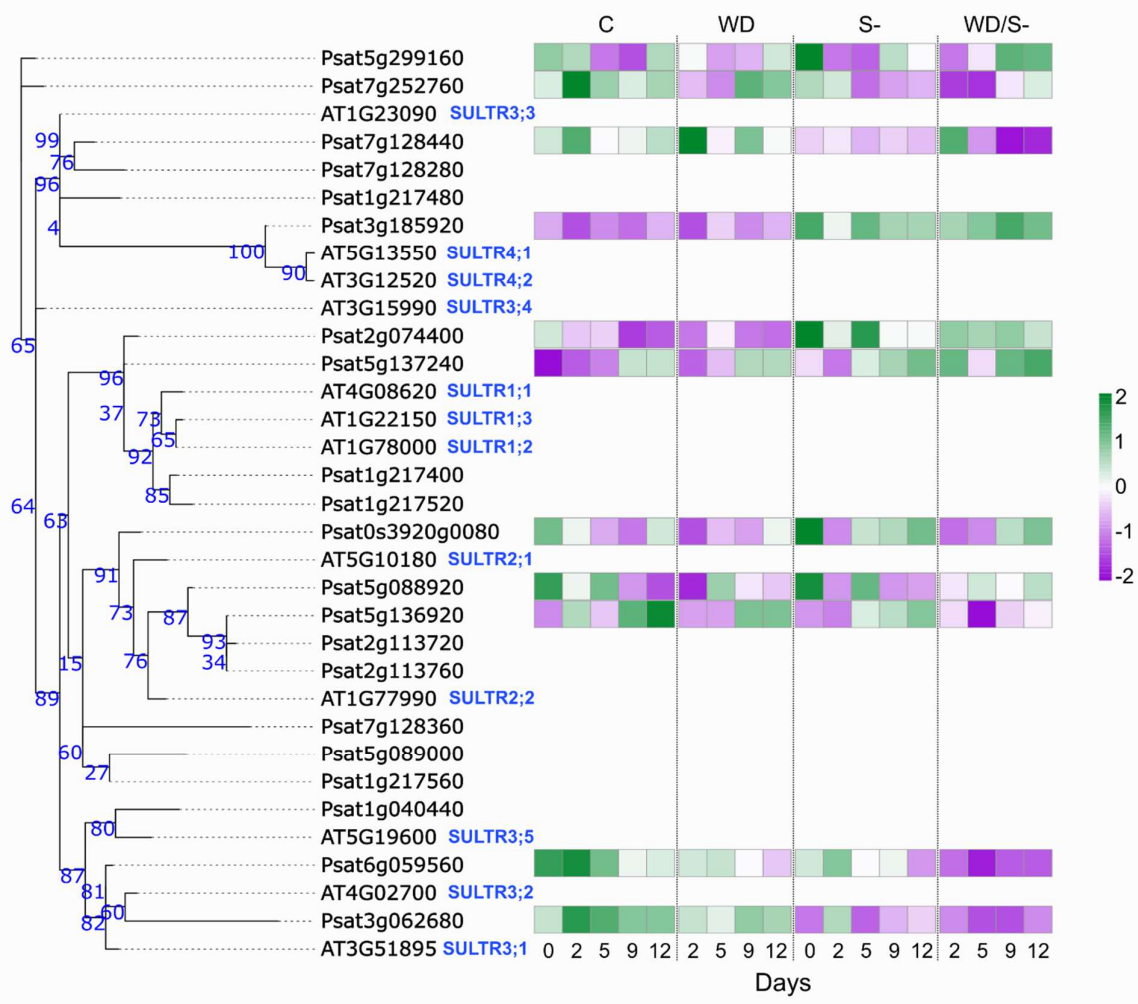

Supplemental Figure S7. Response to stress of sulfate transporters. Phylogenetic tree of sulfate transporters was built using the interactive phylogenetics module of the Dicots PLAZA v5 database (https://bioinformatics.psb.ugent.be/plaza/). Confidence numbers are indicated on the tree branches and provide insights into the reliability of the inferred relationships between sequences. Heatmap represents expression levels of sulfate transporters over time and under control and stress conditions. Data are scaled and are means of n = 4 replicates. Only genes identified as expressed in the experiment and selected for the weighted gene co-expression network analysis are represented. Purple and green colors indicate low and high expression levels, respectively. C: control, WD: water deficit, S-: Sulfur deficiency. Note that day 12 corresponds to three days of rewatering in the WD and WD/S- conditions.

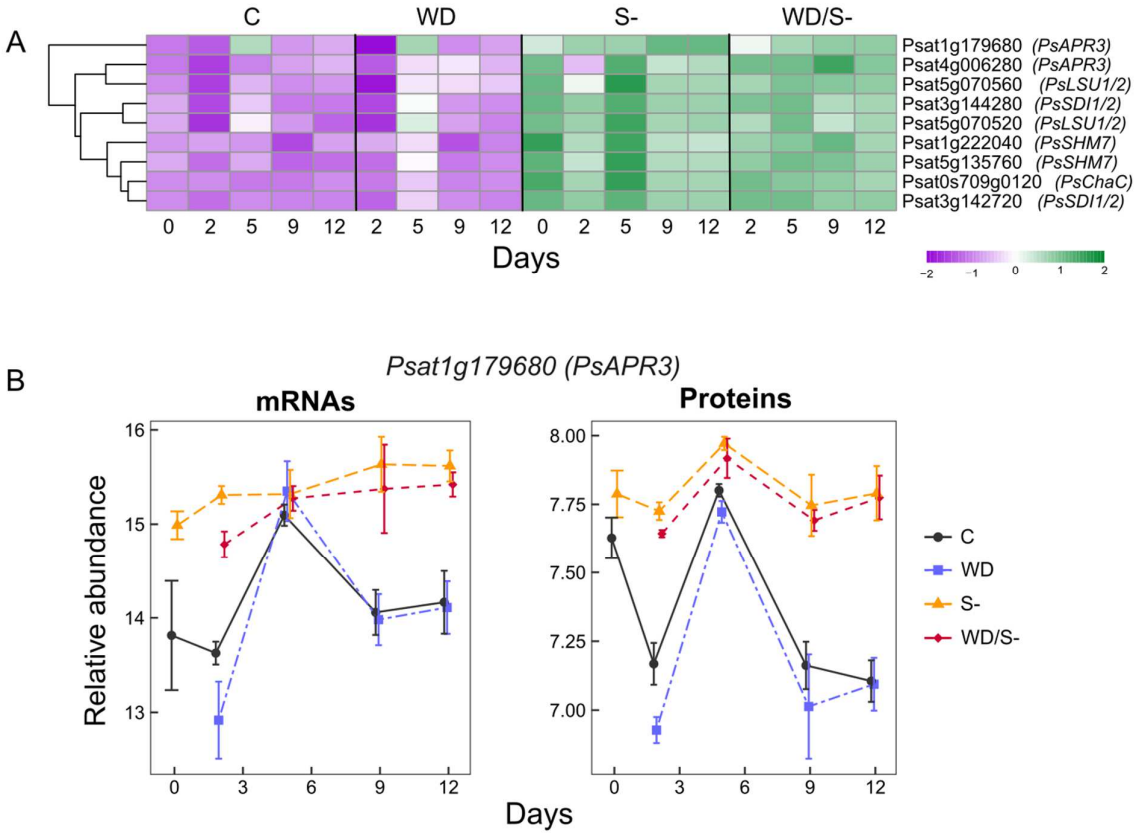

Supplemental Figure S8. Response to stress of OAS cluster genes. A, Heatmap representing expression levels of OAS cluster genes over time and under control and stress conditions. Best homologous genes of Arabidopsis OAS cluster genes were identified using reciprocal BLASTP. Data are scaled and are means of $n = 4$ replicates. Only genes identified as expressed in the experiment and selected for the weighted gene co-expression network analysis are represented. Purple and green colors indicate low and high expression levels, respectively. C, Expression profile of *Psat1g179680*, which was analyzed at both transcriptome and proteome levels (means ± S.D, $n = 4$ replicates). C: control, WD: water deficit, S-: Sulfur deficiency. Note that day 12 corresponds to three days of rewatering in the WD and WD/S- conditions.

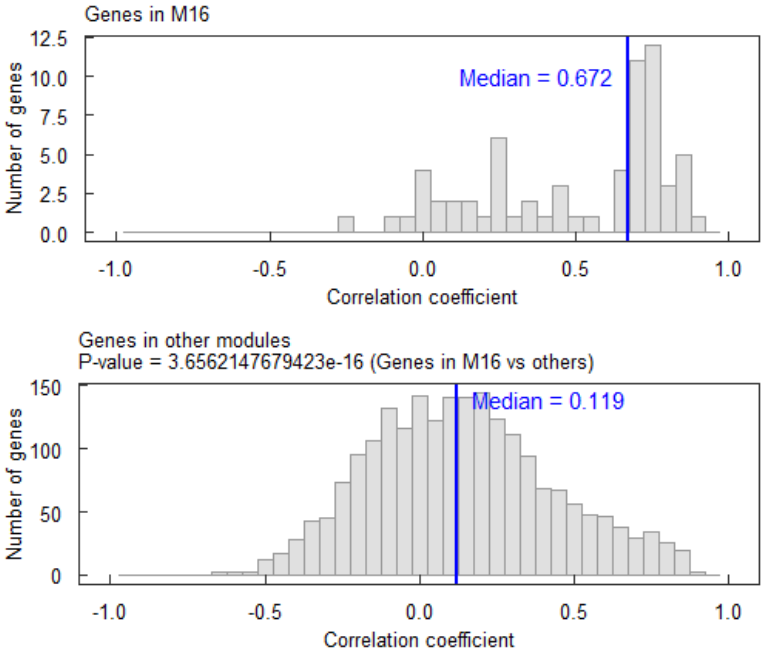

Supplemental Figure S9. Distribution of correlation (Protein vs mRNA, Spearman correlation) coefficients within M16 and other modules. Vertical blue lines indicate medians. The P-value was calculated by comparing correlation coefficients within M16 vs other modules, using a Wilcoxon signed-rank test.

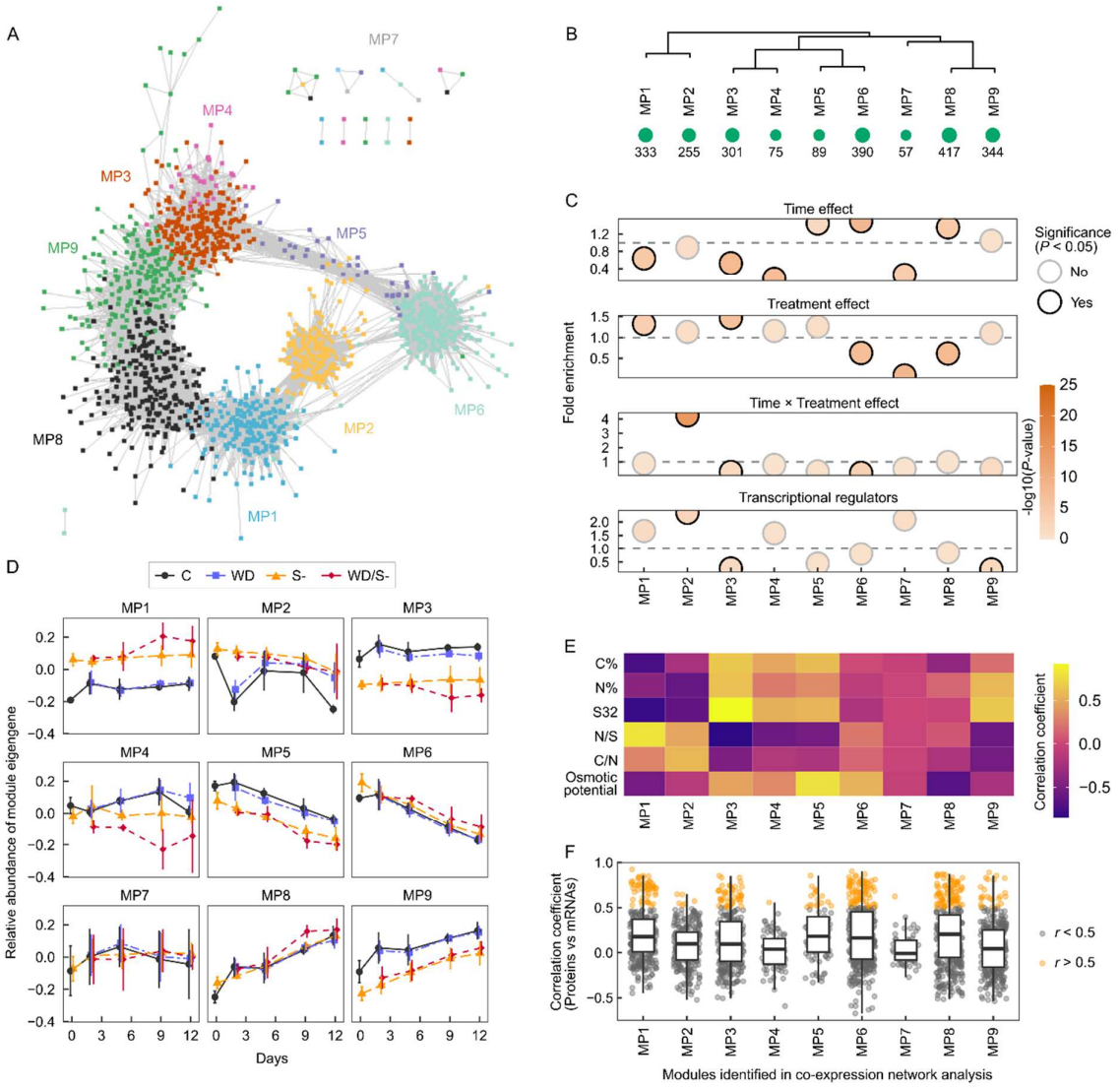

Supplemental Figure S10. Co-accumulation network of proteins reveals modules with distinct patterns of response to stress. A, Co-accumulation network generated with WGCNA and visualized in Cytoscape using a Prefuse Force Directed layout, with an edge threshold cutoff of weight > 0.10. This network was built from proteomics data. Nodes are colored according to their module membership. B, Clustering of module eigengenes. The module eigengene is defined as the first principal component of a given module (Langfelder and Horvath, 2008). Below module names, number of proteins assigned to each individual module are indicated and are represented as bubble plots. C, Bubble plots representing enrichment of specific groups of proteins within each individual module. Fold enrichment < 1 and > 1 correspond to an under- and over-representation in the module, respectively. Proteins with a time, treatment and/or time × treatment interaction effects were identified in Fig. 3A. Transcriptional

regulators were identified using the PlantTFCat tool (see methods). D, Profiles of module eigengenes (means ± S.D, *n* = 4 replicates). E, Heatmap representing the correlation (Spearman) between trait data (elements and physiological parameters) and module eigengenes. F, Boxplots showing the distribution by module of correlation coefficients for the comparison protein vs mRNA. Dots represent individual genes. Genes with a correlation > 0.5 (Protein vs mRNA) are highlighted in orange. Boundaries of the boxes represent the 25th and 75th percentiles, and horizontal lines within boxes represent medians. C: control, WD: water deficit, S-: Sulfur deficiency. Note that day 12 corresponds to three days of rewatering in the WD and WD/S- conditions.

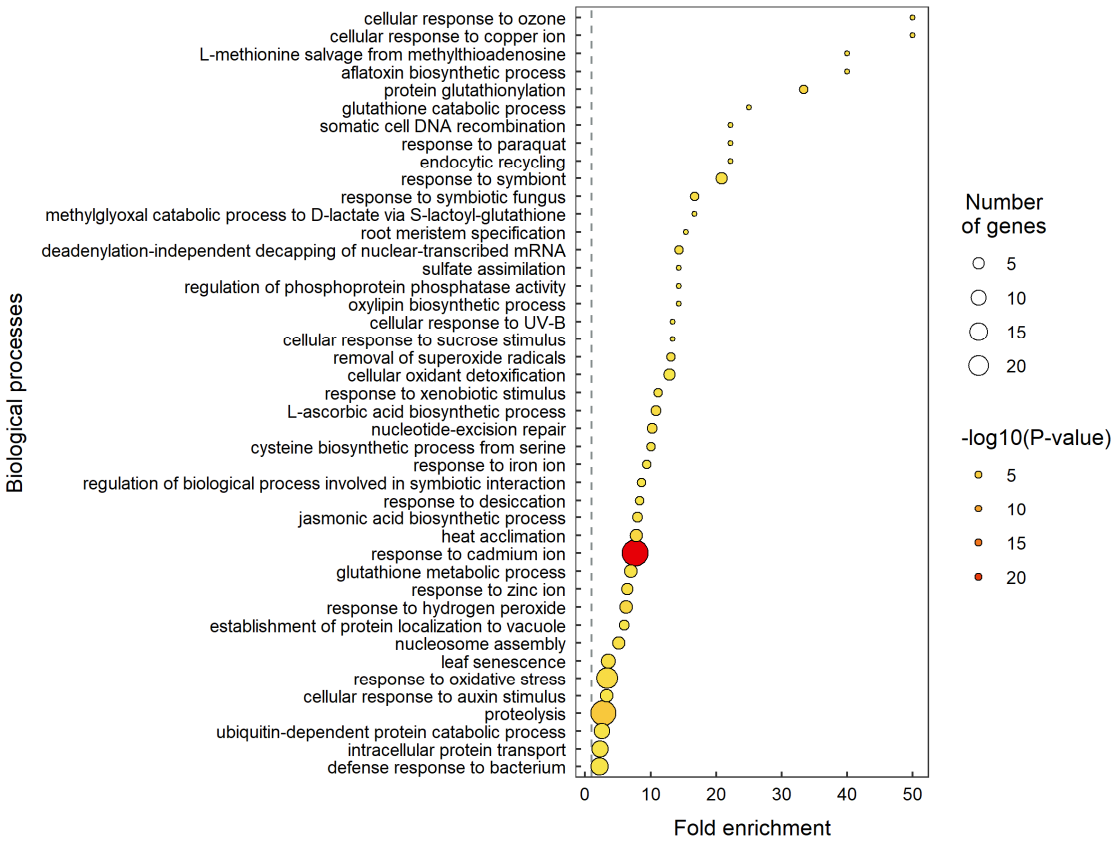

Supplemental Figure S11. Enriched biological processes in the list of 333 proteins grouped in module MP1. Results of the GO enrichment analysis for all modules are provided in Supplemental Data Set S5.

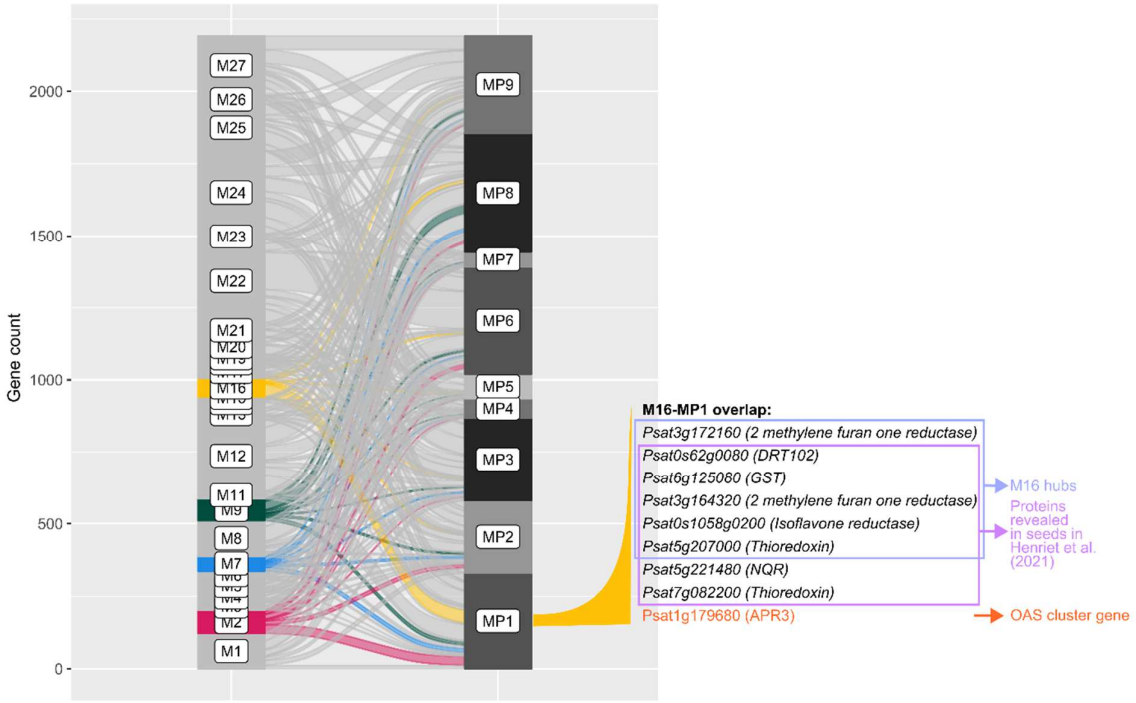

Supplemental Figure S12. Overlap between co-expression modules (transcriptomics data, left) and co-accumulation modules (proteomics data, right). Only genes that were analyzed at both the transcriptome and proteome levels are represented. Module M16 and modules M2/M7/M9, presented in Figures 5 and 6, respectively, are highlighted. Selected genes from the overlap between modules M16 and MP1 are indicated.

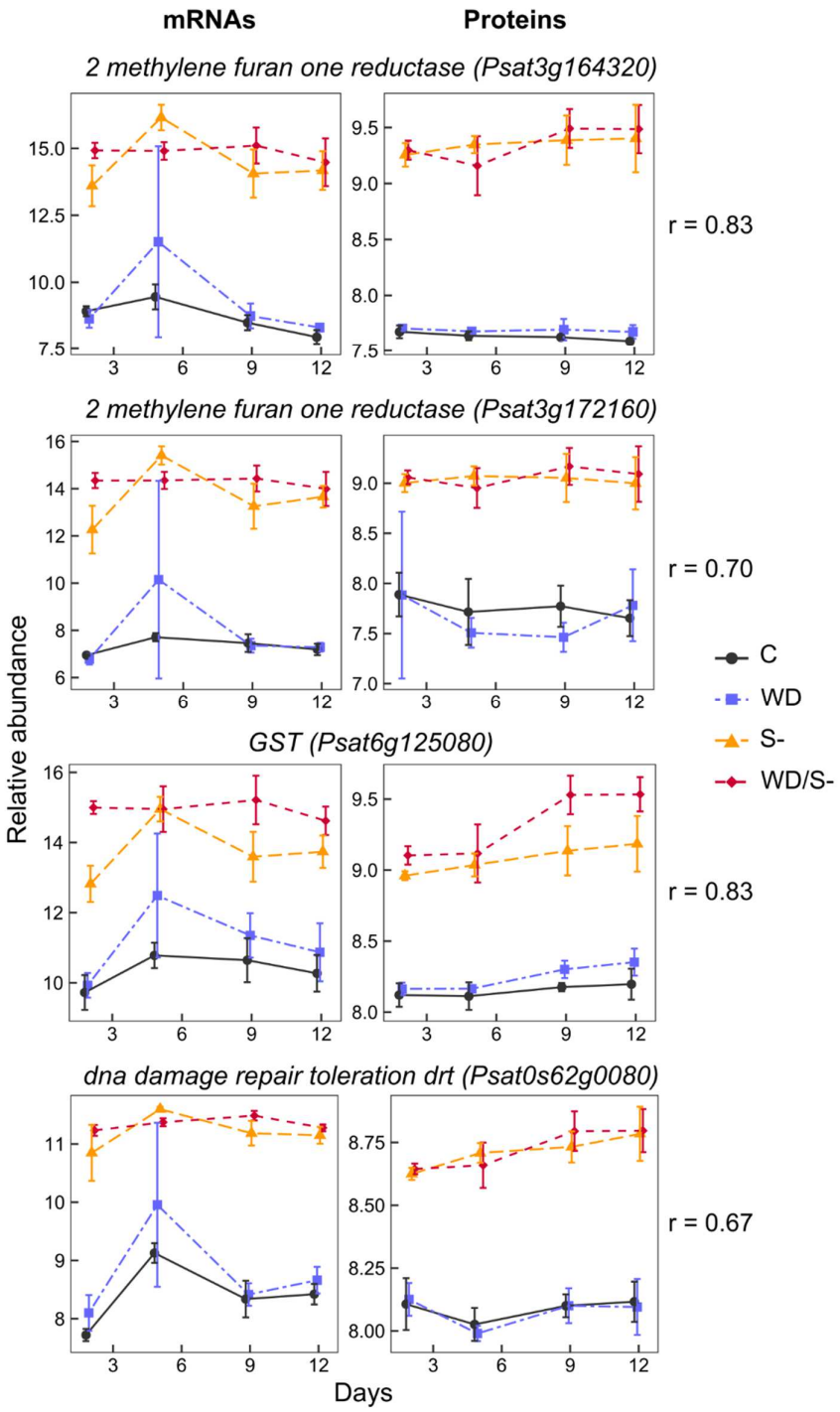

1440

1441 **Supplemental Figure S13**. Expression profiles (mRNAs and proteins) of selected
1442 hubs in module M16 (means ± S.D, *n* = 4 replicates). Correlation (Spearman)
1443 coefficients for the comparison protein vs mRNA are indicated next to the plots. C:
1444 control, WD: water deficit, S-: Sulfur deficiency. Note that day 12 corresponds to three
1445 days of rewatering in the WD and WD/S- conditions.

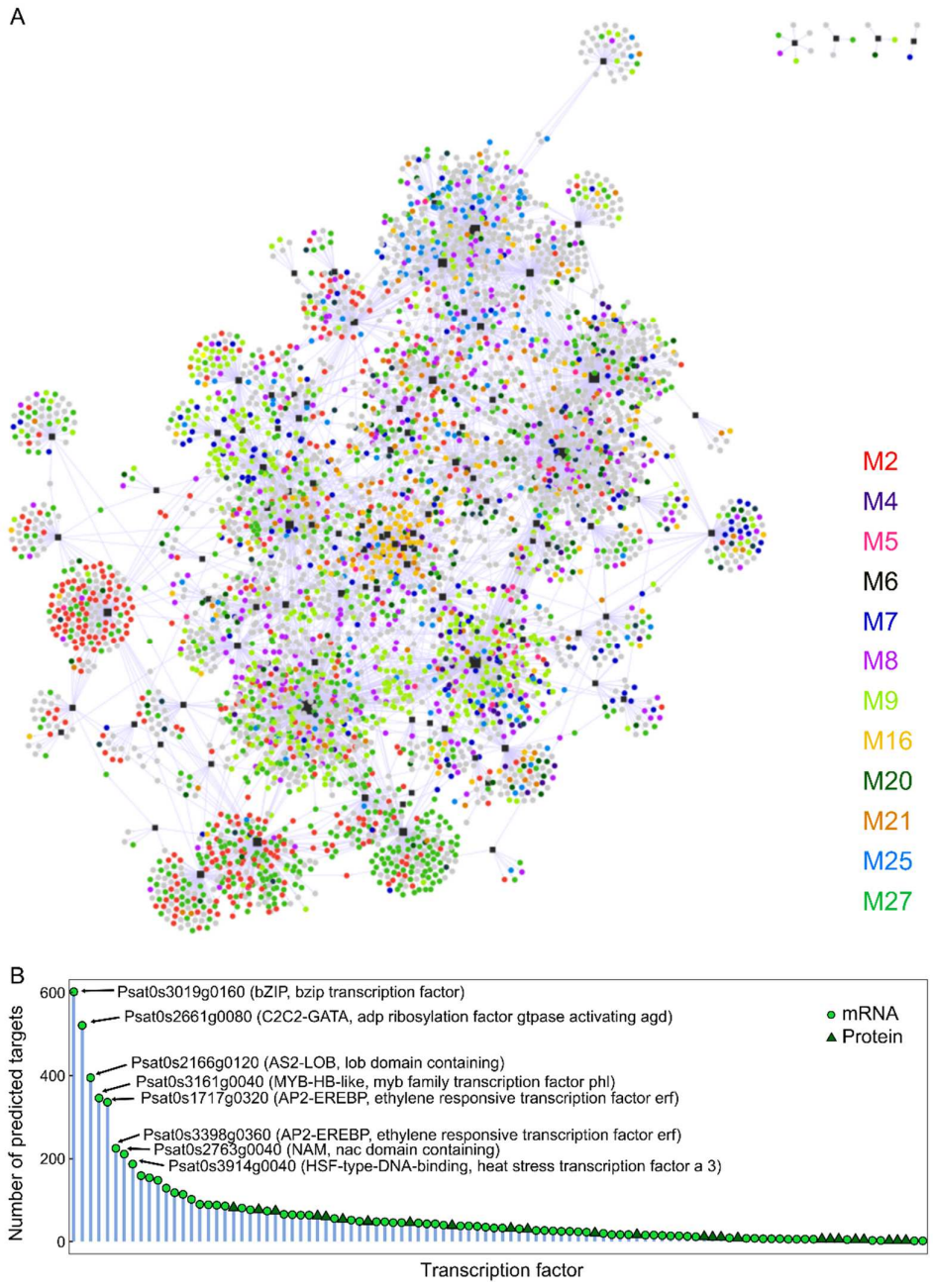

Supplemental Figure S14. Prediction of regulatory connections between TFs and their target genes. A, Gene regulatory network. Edges correspond to regulatory connections predicted with the tool dynGENIE3, and are oriented from regulators to target genes. Regulators are TFs and correspond to proteins or mRNAs (when data for the transcription factor was not available at the proteome level). Targets correspond to mRNAs. Regulators are colored in black and targets are colored according to their module membership in the co-expression network presented in Figure 4. B, Regulators ranked by their number of predicted targets.

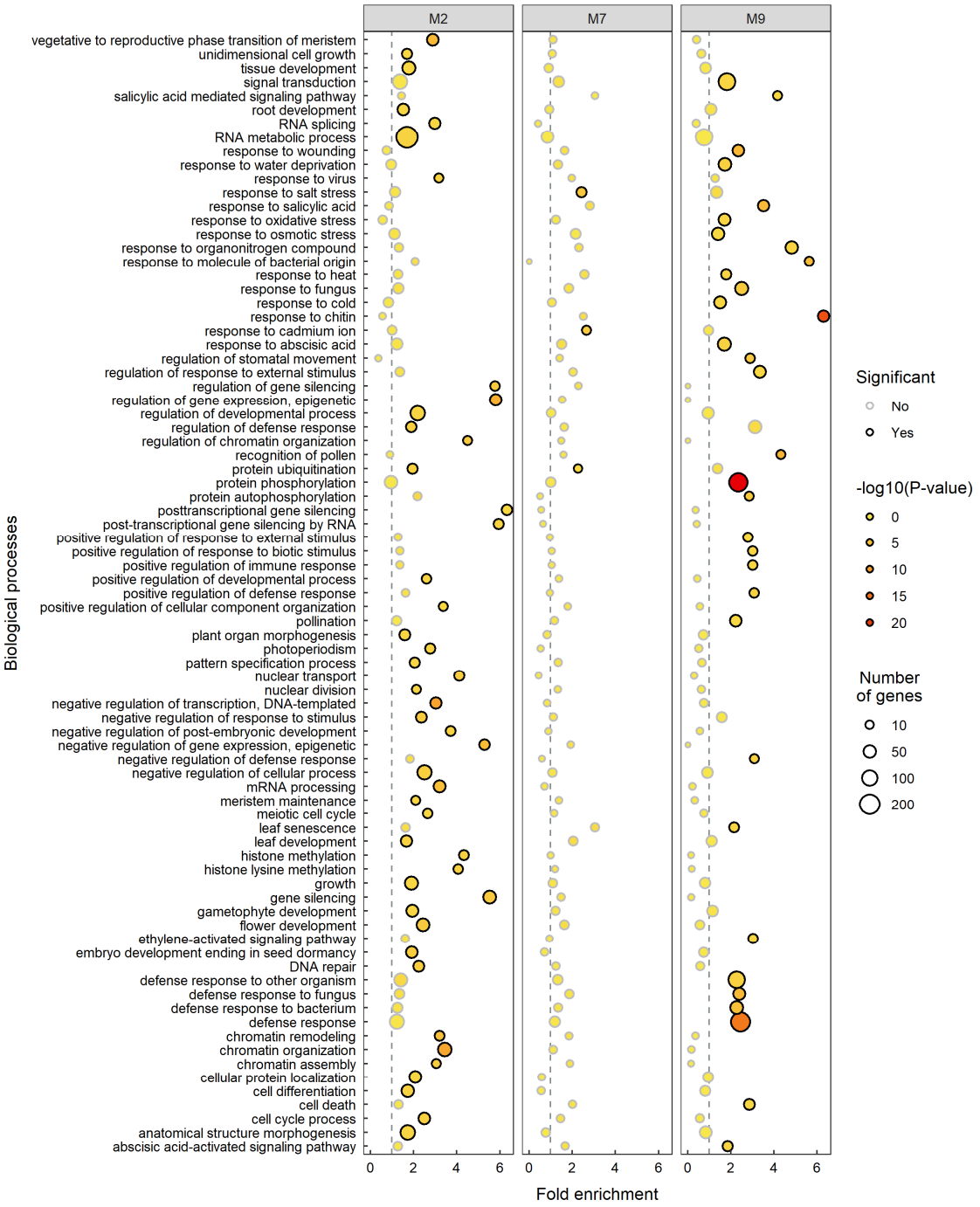

1455

1456 **Supplemental Figure S15**. Selected enriched biological processes in modules M2
1457 (1368 genes), M7 (478 genes) and M9 (1578 genes). Selected processes were
1458 significantly over-represented in any of the three modules, with a minimum of 15 genes.
1459 Results of the GO enrichment analysis are provided in Supplemental Data Set S5.

1460

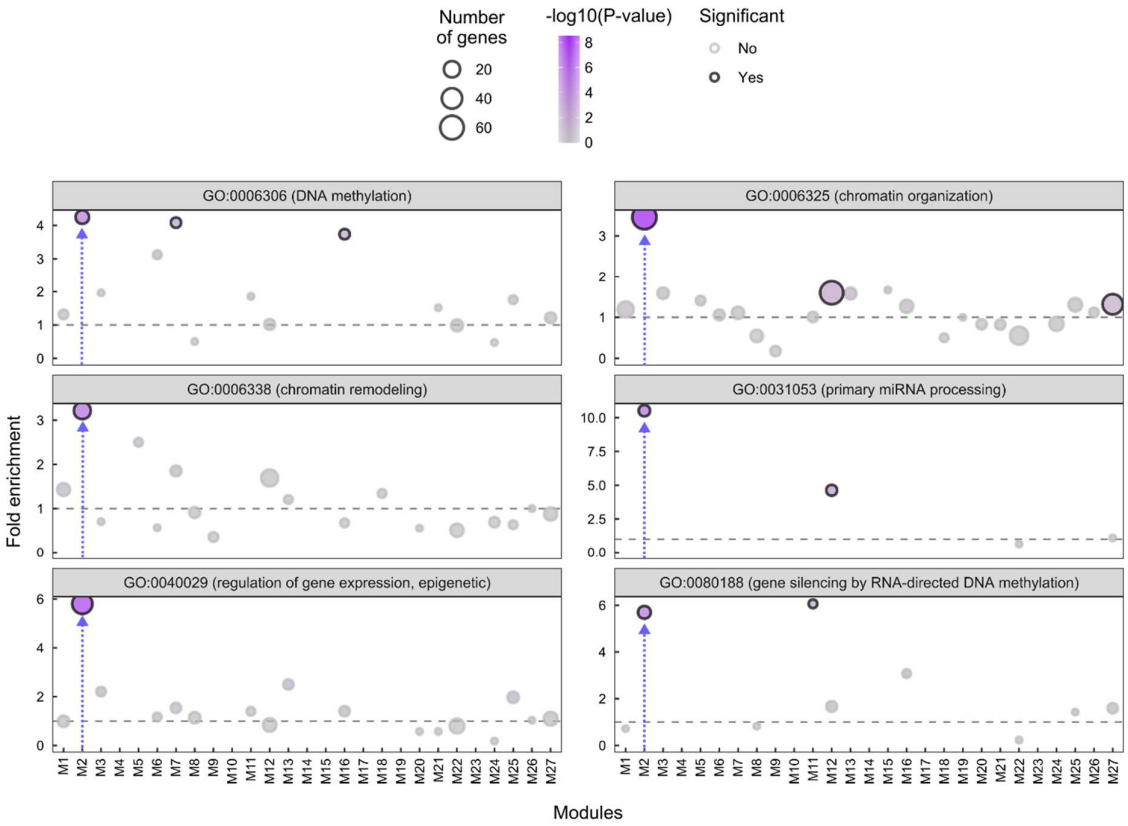

Supplemental Figure S16. Enrichment of biological processes related to epigenetic mechanisms in co-expression modules. Vertical blue arrows indicate enrichment in module M2. Results of the GO enrichment analysis are provided in Supplemental Data Set S5.

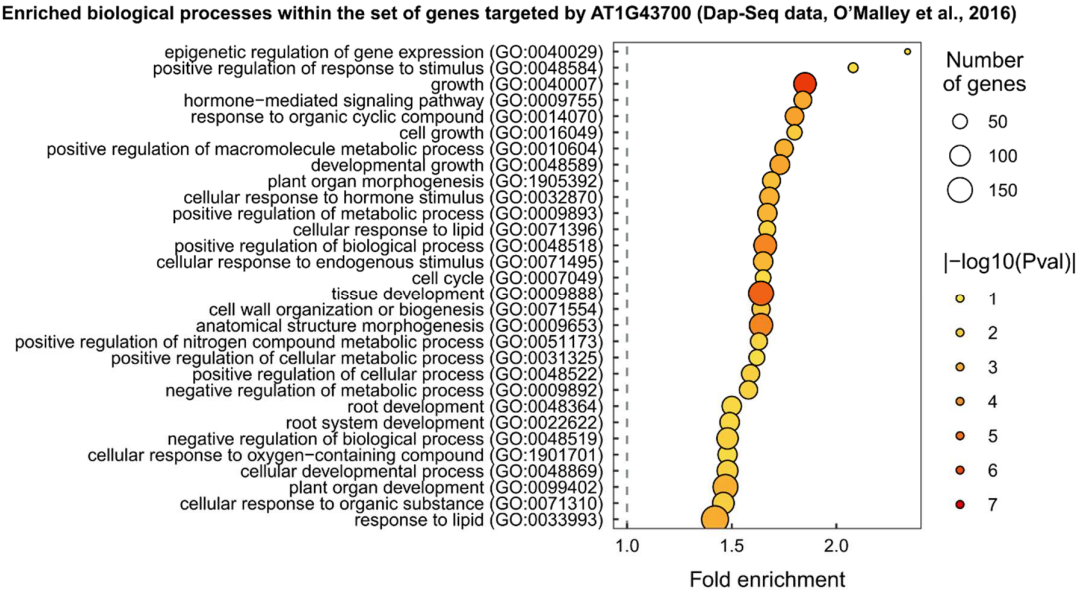

Supplemental Figure S17. Enriched biological processes within the list of genes targeted by AT1G43700, identified as homologous to the regulator R1. Only the top 30 enriched processes (based on fold enrichment values) are represented. Targets of AT1G43700 were identified using the DAP-Seq data produced by O'Malley et al. (2016).